


# Drought-induced tree mortality in Scots pine mesocosms promotes changes in soil microbial communities and trophic groups

**Journal Article****Author(s):**

Jaeger, Astrid C.H.; [Hartmann, Martin](#) ; [Feola Conz, Rafaela](#) ; Six, Johan; Solly, Emily F.

**Publication date:**

2024-02

**Permanent link:**

<https://doi.org/10.3929/ethz-b-000646227>

**Rights / license:**

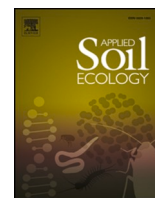
[Creative Commons Attribution 4.0 International](#)

**Originally published in:**

Applied Soil Ecology 194, <https://doi.org/10.1016/j.apsoil.2023.105198>

**Funding acknowledgement:**

180030 - When trees die: Understanding how plants and microbes interact and influence soil biogeochemical processes (SNF)



## Research paper

# Drought-induced tree mortality in Scots pine mesocosms promotes changes in soil microbial communities and trophic groups

Astrid C.H. Jaeger<sup>a,\*</sup>, Martin Hartmann<sup>a</sup>, Rafaela Feola Conz<sup>a</sup>, Johan Six<sup>a</sup>, Emily F. Solly<sup>a,b</sup>

<sup>a</sup> ETH Zurich, Department of Environmental Systems Science, Sustainable Agroecosystems Group, Zurich, Switzerland

<sup>b</sup> Helmholtz Centre for Environmental Research - UFZ, Leipzig, Germany



## ARTICLE INFO

## Keywords:

Soil microbiome

Scots pine

Tree mortality

Drought

Mesocosm experiment

DNA metabarcoding

## ABSTRACT

Increased tree mortality related to water limitation is documented for various species at different sites globally. Nevertheless, our understanding of tree mortality effects on soil microbial communities remains scarce. Therefore, we conducted a mesocosm experiment with young Scots pine saplings and natural forest soil with differing drought legacies to follow changes in soil microbial communities during tree mortality. Scots pine saplings were completely deprived of water during the experiment until they died. Shifts in soil microbial communities during tree mortality were assessed by metabarcoding in parallel with measurements of tree vitality and physicochemical soil properties. Drought history influenced the rate at which trees died, although high individual differences were observed. Tree death was accompanied by reduced stomatal conductance, discoloring of needles, increased defoliation, and shrinkage of the stem diameter. Soil  $\text{NO}_3^-$  concentrations increased after tree death, potentially through diminished plant uptake and increased microbial nitrification. Microbial abundance and community composition were affected by tree death and drought legacy. Copiotrophic bacterial taxa decreased during tree mortality, while oligotrophic taxa increased, probably slowing down soil carbon turnover. Fungal saprotrophs decreased, while symbiotrophs, such as ectomycorrhizal (ECM) fungi, increased in abundance, potentially through facultative saprotrophy and as a survival strategy of the trees in the initial phase of dying. Overall, our results indicate that drought-induced tree mortality promotes changes in soil prokaryotic and fungal communities, potentially affecting soil processes in forest ecosystems.

## 1. Introduction

Tree mortality is a natural ecological process (Franklin et al., 1987); however, drought-induced mortality is often a selective force that differentially affects individual trees and rapidly alters the size, age, composition, and spatial structure of forests (Anderegg et al., 2013). Increased mortality attributed to water limitation has been observed for various tree species (Allen et al., 2010; Hartmann et al., 2022; Klein and Hartmann, 2018; Martínez-Vilalta et al., 2010; Mueller et al., 2005; Rigling et al., 2013) and recent declines in forest productivity and tree survival have been documented at many sites globally (Allen et al., 2010, 2015; Etzold et al., 2019; Zhao and Running, 2010). Drought-associated mortality results from the inhibition of water transport through the vasculature of trees and the imbalance between carbohydrate supply and demand by living tissues (Adams et al., 2013, 2017a; Hartmann, 2015; McDowell, 2011; McDowell et al., 2013, 2022). The

impairments of these physiological mechanisms strongly affect the maintenance of osmotic, metabolic, and carbon-dependent defense requirements by trees (Adams et al., 2017b; McDowell et al., 2008, 2022). Furthermore, increased susceptibility to pests and pathogens has been observed to lead to drought-induced tree mortality (e.g., Anderegg et al., 2015; Desprez-Loustau et al., 2006; Goodman et al., 2013; Oliva et al., 2014; Xiong et al., 2011). In addition to the dieback of mature trees, high mortality levels during sapling development represent a significant bottleneck to recruiting new seedlings into the next forest generation (MacAllister et al., 2019). Thus, getting a better understanding of the resistance of young trees to drought stress is relevant for forest regeneration (Rigling et al., 2013).

Tree mortality and tree decline can affect fluxes of water and nutrients through the plant and soil system (Anderegg et al., 2016; Avila et al., 2016; Avila et al., 2021) and thereby induce changes in soil physicochemical properties (Anderegg et al., 2013; Custer et al., 2020;

\* Corresponding author at: Universitätstrasse 2, Zurich CH-8092, Switzerland.

E-mail addresses: [astrid.jaeger@usys.ethz.ch](mailto:astrid.jaeger@usys.ethz.ch) (A.C.H. Jaeger), [martin.hartmann@usys.ethz.ch](mailto:martin.hartmann@usys.ethz.ch) (M. Hartmann), [rafaela.conz@usys.ethz.ch](mailto:rafaela.conz@usys.ethz.ch) (R.F. Conz), [johan.six@usys.ethz.ch](mailto:johan.six@usys.ethz.ch) (J. Six), [emily.solly@usys.ethz.ch](mailto:emily.solly@usys.ethz.ch) (E.F. Solly).

<https://doi.org/10.1016/j.apsoil.2023.105198>

Received 15 August 2023; Received in revised form 10 November 2023; Accepted 11 November 2023

Available online 21 November 2023

0929-1393/© 2023 The Authors. Published by Elsevier B.V. This is an open access article under the CC BY license (<http://creativecommons.org/licenses/by/4.0/>).

Fontaine et al., 2007; Prescott, 2010). For instance, reduced nutrient uptake by dying trees can increase soil nutrient pools (Cigan et al., 2015; Custer et al., 2020), and diminished uptake of water by decaying trees can result in higher soil water contents (Cigan et al., 2015; Custer et al., 2020). Furthermore, the nutrient cycling within affected forest ecosystems might be modified by changes in plant-derived carbon (C) input as leaf- and root-litter and root exudates (Nave et al., 2011). An observed shift toward a more neutral pH is likely driven by the cessation of rhizodeposits following tree death containing organic acids that leach from the rhizosphere into the bulk soil, lowering the pH (Custer et al., 2020).

Changes in environmental conditions during tree mortality events can, in turn, have a strong effect on the soil microbiome and microbially mediated soil processes (Allsup et al., 2023; Baldrian et al., 2023). Studies, e.g., by Custer et al. (2020) and Yuste et al. (2012), suggest that due to the absence of belowground inputs, tree mortality events can trigger microbial decomposition of soil organic matter (SOM), driving essential changes in the nutrient cycling. For example, nitrogen (N) mineralization rates are expected to increase through inputs of N-rich needle litter and breakdown of N-rich proteins (Edburg et al., 2012; Jenkins et al., 1999; Xiong et al., 2011), whereas root dieback acts as a new source of C to fuel microbial decomposition processes (Solly et al., 2015; Zeller et al., 2008). Furthermore, decreased canopy cover in mortality-affected stands contributes to increased solar radiation and precipitation reaching the soil, supporting decomposition that can lead to decreased soil C:N ratios (Custer et al., 2020). Moreover, studies suggest that tree dieback negatively affects the C sequestration capacity of forest ecosystems (Edburg et al., 2012; Rodríguez et al., 2017; Xiong et al., 2011; Yuste et al., 2011) as an increase in C emissions from microbial heterotrophic respiration during decomposition of dead plant material and roots of dead trees is expected (Anderegg et al., 2013; Hicke et al., 2012; Kurz et al., 2008; Liu et al., 2023). The response of the soil microbiome during tree mortality is tightly linked to the composition of microbial communities; however, our current knowledge of how tree dieback shapes fungal and bacterial communities remains scarce.

Soil fungi comprise a wide range of life strategies ranging from symbiotic to saprotrophic and pathogenic (Nilsson et al., 2019a; Tedersoo et al., 2014), and diverse fungal communities are likely to respond with different sensitivities to tree mortality. Under tree mortality, a change in nutrient availability is expected as readily available root exudates are replaced by an increased input of dead plant material (Štursová et al., 2014). In coniferous forests, under the termination of photosynthate allocation as a result of tree death, symbiotic ECM fungi are expected to decrease, while saprotrophic fungi may increase, benefitting from increased amounts of dead organic matter for consumption, whereas no clear pattern seems to exist for soil fungal pathogens (Hopkins et al., 2018; Rodríguez-Ramos et al., 2021; Štursová et al., 2014; Veselá et al., 2019). Soil bacteria can also present different life strategies, such as copiotrophy – which refers to organisms that preferentially metabolize labile organic C sources such as root exudates – and oligotrophy – which refers to organisms that can survive with alternative types and availabilities of more recalcitrant C resources – (Fierer et al., 2007), which might relate to different responses during an episode of tree mortality.

Drought legacies have been observed to shape the composition of soil microbial communities (Fuchslueger et al., 2016; Göransson et al., 2013; Meisner et al., 2018). Despite this improved understanding, it remains uncertain whether the drought history of soils can also influence the response of the soil microbiome during drought-induced tree mortality events. Previous studies rather focused on the effect of tree decline, tree girdling, stump removal, secondary succession, and tree mortality induced by insect infestations on soil microbial communities (e.g., Gómez-Aparicio et al., 2022; Lloret et al., 2015; Michas et al., 2021; Modi et al., 2021; Yuste et al., 2012). Nevertheless, understanding the changes in soil microbial communities following drought-induced tree death is crucial for predicting changes in soil biogeochemical processes and related changes in edaphic soil physicochemical properties relevant

to vegetation regeneration (Anderegg et al., 2016; Rigling et al., 2013).

Thus, we conducted a mesocosm experiment with young Scots pine saplings and natural forest soil to follow changes in soil microbial communities during a tree mortality event. Scots pine saplings, which had been grown for two years under different water limitation treatments, were completely deprived of water until they died, and shifts in soil microbial communities during this event were assessed by metabarcoding along with measuring plant vitality parameters and soil physicochemical properties. The study's main goal was to examine whether tree death has contrasting impacts on fungal and prokaryotic communities and to identify the effect of drought legacy on post-tree-death community changes.

We hypothesized that (i) tree mortality induces alterations in the structure of fungal and prokaryotic communities, (ii) tree death has contrasting effects on fungal groups with an increase of saprotrophic fungi and a decrease of symbiotic fungi (such as ECM), (iii) tree death will increase the abundance of oligotrophic and decrease the abundance of copiotrophic bacterial taxa, and (iv) drought legacy influences the observed changes in community composition, where soils with the same drought history inherit similar structured microbial communities.

## 2. Material and methods

### 2.1. Experimental set-up

The mesocosms were set up as described in Jaeger et al. (2023a) and Solly et al. (2023). In brief, forest soil (sand/silt/clay %: 49/43/8, skeletal material: 20–50 %) was collected from a mature xeric forest stand dominated by Scots pine trees in the Rhone valley (Pfywald, Canton Valais, Switzerland, 600 m a.s.l.). In September 2019, 18 three-year-old Scots pine (*Pinus sylvestris* L.) saplings were planted with homogenized natural forest soil in pots (32 cm height x 69 cm diameter, 100 L volume) in two greenhouses at the Research Station for Plant Sciences Lindau (ETH Zurich, Switzerland). For three months, the mesocosms were watered twice weekly with 2 L of local rainwater reaching a volumetric water content (VWC) of approximately 30 % (close to field capacity, which was ~35 % VWC). In January 2020, the mesocosms were assigned to three different watering treatments in a randomized design to minimize spatial effects (i.e., variability in light availability). The three levels of watering were: Sufficient water supply (control; 30 % VWC;  $n = 6$ ), decreased amount of water (intermediate; 40 % reduction in VWC of control;  $n = 6$ ), and water stress (severe; 75 % reduction in VWC of control;  $n = 6$ ). These treatments were maintained for 2 years until September 2021. After 2 years, the watering was stopped for all mesocosms simultaneously, and the saplings were completely deprived of water until they died. The greenhouse temperatures were controlled to account for seasonal changes in temperature according to climatological data measured at the MeteoSwiss meteorological station of Sion (Canton Valais, Switzerland), close to where the forest soil used for the mesocosms was collected. Greenhouse temperatures and humidity were constantly monitored (Supplementary Fig. 1C, D). The mesocosms had soil sensors measuring VWC and soil temperature every 60 min (Teros 11, METER Group, Pullman, WA, United States).

### 2.2. Tree parameters

Every month after the stop of the watering, tree height, and stem diameter were measured as proxies of aboveground plant biomass. The height, including the buds, was measured, the diameter was measured at two angles, and the mean was taken. The litterfall was collected during the whole investigation period on a polyethylene net (mesh size 3 mm × 3 mm) placed above the soil surface and pooled together over periods of 3 months. The pooled litter was weighed, dried for one week at 40 °C, and redistributed on the soil surface. Stomatal conductance was measured two weeks after the stop of the watering and then weekly with

an SC1 leaf porometer – stomatal conductance (METER Group) to assess plant water status and the degree of stomata opening and leaf gas exchange as an indicator of plant vitality until the trees reached the vitality status ‘non-vital’ (see below). Each week, stomatal conductance was measured 3 times on the tree’s crown under local radiation, humidity, and temperature, and the mean of these measurements was taken. In a water-limited environment, crown transparency can be used as a proxy for the impact of stresses on the tree, especially of drought events (Carnicer et al., 2011; Eilmann et al., 2013; Sánchez-Salguero et al., 2012). Therefore, visual inspection of the trees’ transparency (defoliation, following Dobbertin et al. (2004); Dobbertin and Brang (2001)) and needle color (as an indication of senescence) was performed weekly. Tree defoliation was defined as the deviance of the foliage of a tree from the full foliage at the status ‘vital’ (0 % defoliation) when trees still received water (following Hunziker et al., 2022). The tree status ‘non-vital’ was defined based on measured stomatal conductance  $\leq 5 \mu\text{mol m}^{-2} \text{s}^{-1}$  at two consecutive weekly measurements (to rule out the influence of light conditions), browning of needles, and defoliation of  $\geq 75\%$ .

### 2.3. Soil sampling

For this study, the first bulk soil sampling was performed in all pots ( $n = 18$ ) when the mesocosms were still watered in autumn-21 (subsequently termed ‘vital’). The second sampling was done individually for

each mesocosm when the trees reached the ‘non-vital’ status (Fig. 1). The last sampling was performed 4 months after the second sampling (‘non-vital’), and the status is hereafter termed ‘dead’ (Fig. 1). The soil sampling was performed with a stainless-steel auger with a 5.5 cm inner diameter down to 15 cm soil depth. The holes in the mesocosm systems produced by the sampling were filled with sterilized sand to minimize soil disruption within the pot.

### 2.4. Physicochemical soil characteristics

The fresh soil samples were sieved to 4 mm on each sampling day, and organic residues  $>2$  mm were sorted out manually. A subsample (0.250 g of soil) for DNA extraction was stored at  $-20^\circ\text{C}$  until further analysis. Fresh soil samples were used to analyze gravimetric water content (GWC, 10 g of soil) and inorganic nitrogen ( $\text{NH}_4^+$ ,  $\text{NO}_3^-$ , 10 g of soil). The rest of the soil samples were dried at  $40^\circ\text{C}$  to constant weight and sieved to 2 mm for measurements of soil pH, total carbon (TC), inorganic carbon (IC), organic carbon content ( $\text{C}_{\text{org}}$ ), and total nitrogen content (TN). The GWC of the soil was assessed by weighing a subsample of 10 g of the soil before and after drying at  $105^\circ\text{C}$  for at least 48 h. Ammonium ( $\text{NH}_4^+$ ) and nitrate ( $\text{NO}_3^-$ ) concentrations of the soils were determined by extracting 10 g soil with 50 mL 2 M KCl solution in a 1:5 soil:solution ratio and shaking for 1 h at 180 rpm. After filtering through a 150 nm ashless filter paper (Whatman No. 42), the extract was stored at  $-20^\circ\text{C}$  until further analyses.  $\text{NH}_4^+$  and  $\text{NO}_3^-$  concentrations were

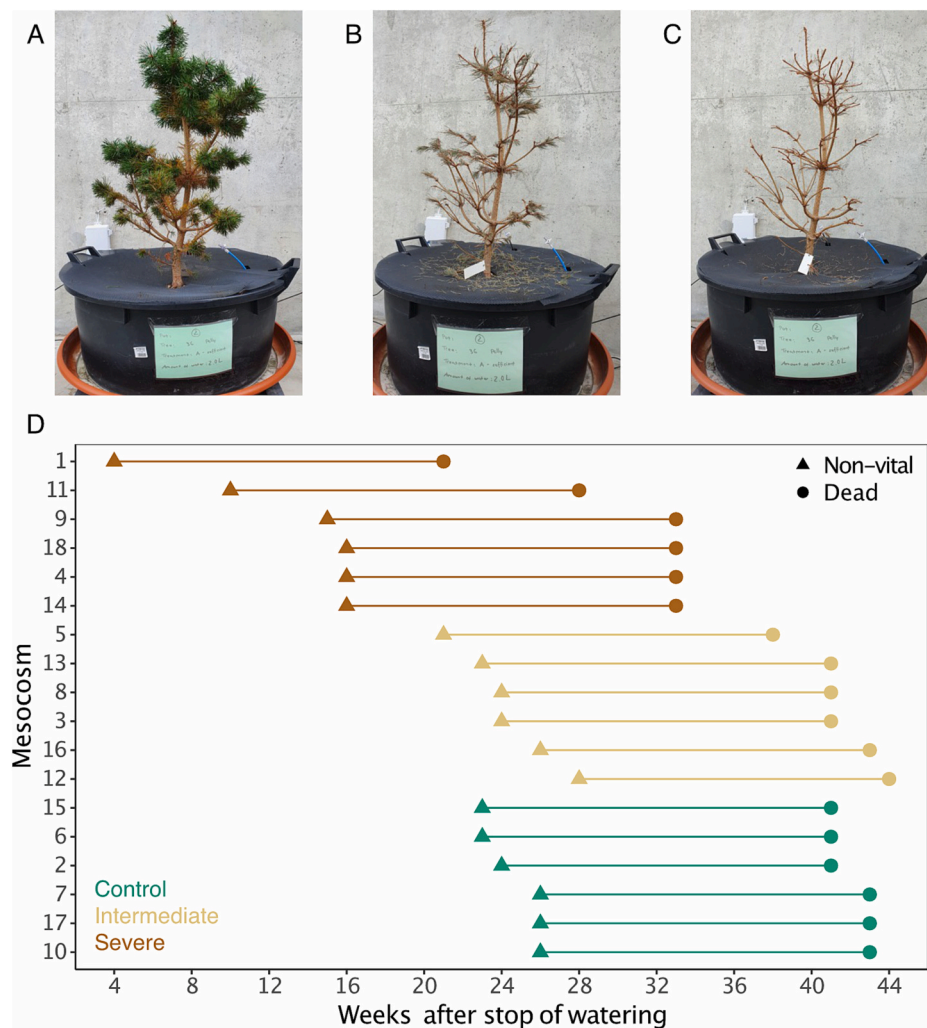


**Fig. 1.** Example for the visual inspection of defoliation for the tree vitality status ‘vital’ (A), ‘non-vital’ (B), and ‘dead’ (C) from a control mesocosm. (D) Individual sampling scheme for all mesocosms ( $n = 18$ ) for the vitality status ‘non-vital’ (triangle) and consecutively ‘dead’ (circle) 16 weeks later.

determined colorimetrically with a spectrophotometer v-1200 (VWR, Radnor, PA, United States) following Forster (1995) for  $\text{NH}_4^+$  and Doane and Horwath (2003) for  $\text{NO}_3^-$ . Soil pH was measured in a 1:2.5 solution containing 10 g of dried soil and 25 mL of 0.01 M  $\text{CaCl}_2$  solution. Samples were shaken horizontally at 180 rpm for 1 h and stored overnight to allow sedimentation before measurement with a pH meter (VWR, Radnor, PA, United States). Total carbon and nitrogen concentrations were determined on milled soil samples with an elemental analyzer LECO 628 (LECO, St. Joseph, MI, United States). Inorganic carbon (IC) was measured with the pressure-calculator method following Sherrod et al. (2002). The organic carbon ( $C_{\text{org}}$ ) was calculated as  $C_{\text{org}} = \text{TC} - \text{IC}$  and used to determine  $C_{\text{org}}/\text{TN}$ , referred to as C:N ratio.

## 2.5. Microbial gene abundance

For DNA extraction from 0.250 g fresh soil, the DNeasy® PowerSoil® Pro Kit (Qiagen, Hilden, Germany) was used according to the manufacturer's instructions with the QIAcube System (Qiagen). The quality and quantity of extracted DNA were measured via UV/VIS spectrophotometry with the QIAxpert System (Qiagen). Extracted DNA was diluted to 2 ng  $\mu\text{L}^{-1}$  to reduce inhibition. Potential amplification inhibition induced by unintentional co-extraction of contaminants was tested across all samples by spiking pGEM-T plasmid (GenBank® Accession No. X65308; Promega, Madison, WI, United States) into the soil DNA at equimolar concentrations in all samples and amplifying a region on the plasmid using the specific primers SP6 and T7 (Microsynth, Balgach, Switzerland). As previously reported (Jaeger et al., 2023a), the abundance of taxonomic groups (bacteria, archaea, fungi) was assessed using a SYBR® Green-based qPCR approach. The qPCR standards were produced from purified PCR products obtained by pooling DNA from randomly selected samples. For all reactions, standard curves were obtained from diluted standards with concentrations ranging from  $10^{-2}$  to  $10^{-8}$  ng of DNA template, and a negative control containing ddH<sub>2</sub>O was used. The selected primers (Microsynth) 515F (Parada et al., 2016) and 806R (Frey et al., 2016) targeted the 16S rRNA gene (V4 region). The primers FF390 (nu-SSU-1334-5') and FR1 (nu-SSU-1648-3') (Vainio and Hantula, 2000) were chosen to target the 18S rRNA gene of fungi (V7-V8 region). All qPCR reactions were performed in a final volume of 25  $\mu\text{L}$  containing a final concentration of 0.75  $\mu\text{M}$  of primer,  $1 \times$  Sso Advanced™ Universal SYBR® Green Supermix (Bio-Rad Laboratories, Hercules, CA, United States), and 10 ng of DNA template. The conditions for the qPCR assays were as follows: 3 min for enzyme activation at 98 °C, followed by 15 s for denaturation at 95 °C, 30 s primer hybridization at 52 °C for 16S and 50 °C for 18S, respectively, and 30 s for elongation at 72 °C, for 35 cycles. All qPCRs were performed in technical triplicates in a thermocycler CFX96 Touch Real-Time System (Bio-Rad Laboratories, Hercules, CA, United States). Melting curves were generated to verify the amplification specificity. The same 8 samples were repeated in every plate to check for between-run differences. The CFX Maestro software (Bio-Rad Laboratories, Hercules, CA, United States) was used to document and analyze the results. The estimated numbers of prokaryotic and fungal copies were used to calculate the prokaryotic-to-fungal ratio.

## 2.6. Microbial community structure

Changes in prokaryotic and fungal community structure were investigated with DNA metabarcoding of ribosomal markers, as described in Jaeger et al. (2023a). To reduce inhibition, the extracted DNA was diluted to 20 ng  $\mu\text{L}^{-1}$ . PCR amplification of the prokaryotic 16S rRNA gene (V3–V4 region) was performed using the primers 341F and 806R (Frey et al., 2016). The fungal ITS2 region of the *rnr* operon was targeted using the primers ITS3ngs and ITS4ngs (Tedersoo and Lindahl, 2016). PCR reactions contained  $1 \times$  of GoTaq® G2 Hot start Master Mix from Promega (Promega, Madison, WI, United States), 0.4

$\mu\text{M}$  of the primers, and 40 ng of DNA template in a final volume of 25  $\mu\text{L}$ . Cycling conditions for the PCR reactions consisted of a polymerase activation step at 95 °C for 5 min, followed by denaturation at 95 °C for 40 s, primer hybridization at 58 °C respectively at 55 °C for fungi for 40 s, and elongation at 72 °C for 1 min, repeated in 30 cycles. PCR amplification was carried out in technical triplicates, and triplicates were pooled before sequencing. Pooled PCR products were sent to the Functional Genomics Center Zurich (FGCZ, Zurich, Switzerland) for indexing PCR. Indexed PCR products were purified, quantified, and pooled in equimolar ratios. To achieve optimal read count distributions across all samples, pre-sequencing on the Illumina MiniSeq platform (Illumina, San Diego, CA, United States) was performed to inform library re-pooling. The Illumina MiSeq platform (Illumina) with the v3 chemistry for PE300 reads was used for final sequencing. The raw sequences were deposited in the European Nucleotide Archive (ENA) under the accession numbers PRJEB61158 and PRJEB64205.

## 2.7. Bioinformatics

Sequencing data were processed using a customized bioinformatics pipeline based on VSEARCH v2.22.1 (Rognes et al., 2016). Primers used in PCR were trimmed with CUTADAPT v4.0 (Martin, 2011), allowing for 1 mismatch. Bowtie2 v2.5.1 (Langmead and Salzberg, 2012) was used to filter for PhiX contamination by aligning the reads against the PhiX genome (accession NC\_001422.1). The *fastq\_mergepairs* function in VSEARCH was used to merge trimmed paired-end reads, and the *fastq\_filter* function was applied for quality filtering with a maximum expected error of 1 (Edgar and Flyvbjerg, 2015). Sequences were dereplicated using the *derep\_fulllength* function in VSEARCH and delineated into amplicon sequence variants (ASVs) applying the UNOISE algorithm (Edgar, 2016a) of VSEARCH with an alpha of 2 and a minsize of 8. The UCHIME2 algorithm (Edgar, 2016c) implemented as the *uchime3\_denovo* function in VSEARCH was used to identify and remove potentially chimeric ASV sequences. The remaining ASV sequences were tested for ribosomal signatures using *Metaxa2* v.2.2.3 (Bengtsson-Palme et al., 2015) for the 16S rRNA gene and *ITSx* v.1.1.3 (Bengtsson-Palme et al., 2013) for the ITS2 sequences, and non-matching sequences were discarded. The final ASV table was generated by mapping the quality-filtered reads of each sample against the verified ASV sequences executing the *usearch\_global* algorithm implemented in VSEARCH with the following settings: maxhits 1, maxrejects 100, maxaccepts 0, and a minimum identity of 97 %. Verified ASV sequences were taxonomically classified by running the SINTAX algorithm (Edgar, 2016b) of VSEARCH against the SILVA v.138 database (Quast et al., 2013) for the 16S rRNA gene sequences and the UNITE v.8.3 database (Abarenkov et al., 2010; Nilsson et al., 2019b) for the ITS2 sequences, using a bootstrap cut-off of 0.8. ASVs not assigned to the domain level of bacteria, archaea, or fungi, and ASVs assigned to organelle structures (chloroplasts and mitochondria) were removed from the ASV table.

## 2.8. Statistical analyses

All statistical analyses were computed in R Version 4.3.0 (R Core Team, 2023) using RStudio Version 2023.03.1 (RStudio Team, 2023), and plots were created using ggplot2 v.3.4.2 (Wickham et al., 2023) unless indicated otherwise. A *P*-value < 0.05 was considered significant for all tests unless mentioned otherwise. The data were fitted to linear mixed effect models (lme) to test the effect of the drought legacy and the vitality status on the investigated soil parameters, tree parameters, and microbial gene abundance. Here, the *lme* function of the package nlme v.3.1–162 (Pinheiro et al., 2022) was applied using the restricted maximum likelihood method 'REML' (Meyer, 1989). The drought legacy (DL, control, intermediate, severe) and vitality status (S, vital, non-vital, dead) were used as factor variables with interaction. The greenhouse (greenhouses 1 and 2) and the pot number (pots 1–18) were assumed to be a nested random effect. When visual inspection of residual diagnostic

plots revealed that the data deviated from the normality assumption, the data was transformed. For this transformation, the function  $\log$  (for VWC),  $\log_{10}$  (for  $\text{NO}_3^-$ , 16S gene copies, 18S gene copies, prokaryotic: fungal ratio, stomatal conductance, and litterfall), and  $\sqrt{\text{}}$  (for C:N ratio and tree height) were applied. Estimated marginal means with the *emmeans* function of the package *emmeans* v.1.8.6 were calculated to test the effects of drought legacy and vitality status. Pairwise comparisons were performed by the *contrast* function with the type 'response' of the same package and corrected for multiple testing with the 'sidak' method. The function *cl* of the package *multcomp* v.1.4–23 (Hothorn et al., 2023) was applied to identify and display significant differences between groups. Sequencing depth was investigated and plotted using rarefaction curves with the *rarecurve* function in the *vegan* package v.2.6–4 (Oksanen et al., 2022).

Changes in  $\alpha$ -diversity (Observed richness, Pielou's evenness, and Shannon diversity) and  $\beta$ -diversity (Bray–Curtis dissimilarity) were calculated from 100-fold iteratively subsampled and square-root transformed ASV count tables (Hemkemeyer et al., 2019; Martiny et al., 2017) to account for differences in sequencing depth. Here, the functions *rrarefy*, *specnumber*, *diversity*, and *vegdist* in *vegan* were applied. The effects of drought legacy (DL) and vitality status (S) on  $\alpha$ - and  $\beta$ -diversity were assessed using univariate or multivariate permutational analysis of variance (PERMANOVA; Anderson, 2001) and permutational analysis of multivariate dispersions (PERMDISP; Anderson, 2006) with 999 permutations, as implemented in the *adonis2* and *betadisper* functions of *vegan*. Pairwise comparisons between factor levels were performed using the *pairwise.perm.manova* function from the package *RVAideMemoire* v.0.9-82-2 (Hervé, 2023). Differences in  $\beta$ -diversity were assessed by unconstrained ordination using principal coordinate analysis (PCO) (Gower, 2015) with the *cmdscale* function. Constrained ordination was performed using canonical analysis of principal coordinates (CAP) (Anderson and Willis, 2003) implemented as the *CAPdiscrim* function in the *BiodiversityR* package v.2.15-1 (Kindt, 2008), with 999 permutations, setting the factors drought legacy and vitality status as constraining factors. Here, the CAP reclassification success rate quantitatively estimates the degree of discrimination between groups. The effects of measured physiochemical soil properties and plant parameters on microbial communities were obtained using the PERMANOVA test. Additionally, factors labeled as significant in the PERMANOVA test were further used as a constraining factor in building a parsimony model executing the function *ordistep* in *vegan*, and the significant factors were displayed by distance-based redundancy analysis (db-RDA) (Legendre and Andersson, 1999), using the *dbRDA* function in *vegan*.

The response of individual taxonomic groups from phylum to genus level toward the vitality status was assessed using univariate PERMANOVA based on Euclidean distances via the *adonis2* function with 999 permutations on aggregated data at each taxonomic level, i.e., summing up the read counts of ASVs assigned to the same taxonomic group (Supplementary data). The *qvalue* function of the R package *qvalue* v.2.32.0 (Storey et al., 2023) was used to adjust for multiple testing by calculating *q*-values (Storey and Tibshirani, 2003), and *q*-values < 0.05 were considered significant, and *q*-values < 0.1 as marginally significant. To avoid inflation of type II error due to the impact of rare taxa (low read counts across all samples) on multiple testing corrections, ASVs with an overall abundance < 0.01 % were not included in the test.

The data was scaled (z-transformed) to calculate and visualize changes in relative abundance related to the vitality status. A subset was created for the phyla with a significant ( $q < 0.05$ ) response to the vitality status from the PERMANOVA analysis. The relative change in abundance compared to the vitality status 'vital' was calculated for each responsive phylum. A subset was created for the genera with a significant ( $q < 0.05$ ) response to the vitality status and an overall relative abundance of > 0.1 % from the PERMANOVA analysis. Heatmaps were generated using the *heatmap.2* function of the package *gplots* v.3.1.3 (Warnes et al., 2022) based on z-transformed data to visualize changes

in the relative abundance of genera related to the vitality status. Cluster analysis based on the Ward method (Ward, 1963) was performed to group genera with a similar response structure. Pairwise comparisons between the vitality status were performed with the *pairwise.perm.manova* function as described above to identify significant differences between 'vital' vs. 'non-vital', 'non-vital' vs. 'dead', and 'dead' vs. 'vital' at the genus level.

Fungal ASVs were classified into trophic modes based on FUNGuild v.1.1 (Nguyen et al., 2016) in conjunction with literature research. Only assignments with confidence rankings of 'probable' or 'highly probable' were considered. These data were used to calculate the mean relative abundance of each trophic mode for each vitality status. To test for significant differences between the vitality status for each trophic mode, the *pairwise.perm.manova* function was applied as described earlier.

### 3. Results

#### 3.1. Development of the dying trees

All trees reached the 'non-vital' status based on the measurement of stomatal conductance and visual inspection of defoliation within 28 weeks after the watering was halted (Fig. 1D). Trees previously treated with severe water limitation reached the 'non-vital' vitality status 4–16 weeks after the watering stop (Fig. 1D) and thereby significantly ( $P < 0.001$ ) earlier than the other drought legacies. Trees previously treated with intermediate and sufficient water availability reached the 'non-vital' status only after 20 to 28 weeks, whereby the difference between the drought legacies was not significant. The variability in timing within the intermediate drought legacy was the highest (Fig. 1D).

Until the trees died, the stomatal conductance significantly differed among drought legacies ( $P = 0.0142$ , Table 1). The control trees had the highest stomatal conductance, followed by intermediate and severe (Supplementary Fig. 1B). After the stop of the watering, the stomatal conductance of the trees decreased over time, with the most significant decrease within 4 weeks after the stop (Supplementary Fig. 1B).

Although the trees still slightly grew in the control mesocosms by 1–2 cm even after the stop of the watering (Supplementary Fig. 2A) and tree height was higher in the control, the height of the trees was not affected by the vitality status of the trees (Table 1). On the other hand, tree diameter was significantly affected by the vitality status of the trees ( $P < 0.001$ , Table 1), as the stems of the trees overall decreased in diameter over time by 1–5 mm (Supplementary Fig. 2B). The interaction between tree vitality status and drought legacy also significantly influenced the diameter size of the trees ( $P = 0.0498$ , Table 1). The diameter of the trees in the control mesocosms remained highest throughout this study. Litterfall was higher in the control mesocosms, followed by the intermediate and severe drought legacies (Supplementary Fig. 2C). However, this difference was not significant, and the amount of litterfall did not differ among the vitality status of the trees ( $P = 0.1331$ , Table 1).

#### 3.2. Soil microbial communities

Estimated prokaryotic and fungal ribosomal rRNA gene copy numbers were significantly affected by the vitality status of the trees ( $P < 0.0001$ , Table 1). The abundance of prokaryotes increased throughout the experiment; on the contrary, fungi only increased between the vitality status 'vital' and 'non-vital' (Supplementary Fig. 3A, 3B). Also, the prokaryotic-to-fungal ratio increased throughout the period (Supplementary Fig. 3C) and was significantly affected by the vitality status ( $P < 0.0001$ , Table 1), whereas no differences between drought legacies were found.

Metabarcoding yielded 2'992'951 16S rRNA gene sequences delineated into 28'619 ASVs, and 1'983'308 ITS2 sequences delineated into 2'936 ASVs obtained across 53 samples. Prokaryotic  $\alpha$ -diversity (examined by observed richness, Pielou's evenness, and Shannon diversity) was significantly different among the drought legacies (Table 2); it was

**Table 1**

Effects of drought legacy (DL,  $n = 3$ ), vitality status (S,  $n = 3$ ), and their interaction (SxDL,  $n = 9$ ) on soil physicochemical parameters, abundance, and ratio of taxonomic markers (16S rRNA gene, 18S rRNA gene), and tree parameters tested with linear mixed effect models and displayed with the F-ratio (F) and level of significance (P). Significant results are indicated with bold numbers. VWC = volumetric water content; TC = total carbon concentration;  $C_{org}$  = organic carbon concentration; TN = total nitrogen concentration;  $NH_4^+$  = ammonium concentration;  $NO_3^-$  = nitrate concentration; C:N = soil C:N ratio.

Parameter	Drought legacy (DL)		Status (S)		S × DL	
	F	P	F	P	F	P
VWC	44.84	<b>&lt;0.0001</b>	477.24	<b>&lt;0.0001</b>	59.66	<b>&lt;0.0001</b>
pH	0.40	0.6579	0.70	0.5088	0.40	0.8389
$C_{org}$	0.07	0.9356	5.48	<b>0.0094</b>	1.32	0.2860
TC	0.41	0.6729	5.75	<b>0.0077</b>	1.38	0.2629
TN	0.21	0.8122	34.56	<b>&lt;0.0001</b>	0.22	0.9276
C:N	0.65	0.5353	38.64	<b>&lt;0.0001</b>	1.80	0.1549
$NH_4^+$	0.19	0.8308	3.90	<b>0.0335</b>	0.03	0.9978
$NO_3^-$	0.43	0.6602	30.28	<b>&lt;0.0001</b>	1.75	0.1657
16S gene copies	1.00	0.3800	541.00	<b>&lt;0.0001</b>	0.00	0.9500
18S gene copies	1.00	0.3800	303.00	<b>&lt;0.0001</b>	1.00	0.6900
prokaryotic:fungal copies	1.10	0.3741	535.60	<b>&lt;0.0001</b>	0.20	0.9465
Tree height	3.22	0.0707	3.62	0.0931	1.62	0.1961
Tree diameter	3.52	0.0578	57.49	<b>&lt;0.0001</b>	2.69	<b>0.0498</b>
Stomatal conductance	5.85	<b>0.0142</b>	1169.42	<b>&lt;0.0001</b>	6.19	<b>0.0110</b>
Litter fall	3.09	0.0775	2.16	0.1331	0.87	0.4959

**Table 2**

Effects of drought legacy (DL,  $n = 3$ ), vitality status (S,  $n = 3$ ), and their interaction (SxDL,  $n = 9$ ) on prokaryotic (A) and fungal (B)  $\alpha$ - and  $\beta$ -diversity assessed by univariate ( $\alpha$ -diversity) and multivariate ( $\beta$ -diversity) permutational analysis of variance (PERMANOVA). Values indicate the F-ratio (F), the level of significance (P), and the explained variance ( $R^2$ ). Significant heterogeneities of variance assessed by permutational analysis of univariate dispersion (PERMDISP) are indicated with an asterisk. Significant results are displayed in bold.

	$\alpha$ -Diversity									$\beta$ -Diversity		
	Observed Richness (S)			Pielou's Evenness (J)			Shannon Diversity (H)			Bray-Curtis dissimilarity		
	$R^2$	F	P	$R^2$	F	P	$R^2$	F	P	$R^2$	F	P
<b>(A) Prokaryotes</b>												
Drought legacy (DL)	0.182	6.28	<b>0.005</b>	0.454	25.72	<b>0.001*</b>	0.387	16.69	<b>0.001*</b>	0.199	6.58	<b>0.001*</b>
Status (S)	0.102	3.52	<b>0.043</b>	0.097	5.48	<b>0.006</b>	0.025	1.06	0.373	0.081	2.70	<b>0.001</b>
S × DL	0.081	1.40	0.234	0.060	1.71	0.159	0.078	1.68	0.162	0.056	0.93	0.652*
<b>(B) Fungi</b>												
Drought Legacy (DL)	0.173	5.12	<b>0.006</b>	0.015	0.40	0.650	0.033	0.87	0.430	0.081	2.37	<b>0.001</b>
Status (S)	0.027	0.80	0.458	0.104	2.73	0.073*	0.079	2.05	0.140	0.097	2.83	<b>0.001*</b>
S × DL	0.039	0.57	0.660	0.022	0.29	0.883	0.024	0.32	0.860	0.054	0.79	0.918*

higher under control than intermediate and severe (Supplementary Fig. 4A–C). Furthermore, observed richness and Pielou's evenness were significantly affected by the vitality status of the trees ( $P = 0.043$ ,  $P = 0.006$ , Table 2) and increased toward the vitality status 'dead' except for trees that had been treated with severe water limitation where a decrease over time was observed (Supplementary Fig. 4A, 4C). Fungal observed richness ( $P = 0.006$ ), but not Shannon diversity and Pielou's evenness, were affected by the drought legacy (Table 2), and the highest  $\alpha$ -diversity was observed for the severe drought legacy at all stages of tree vitality (Supplementary Fig. 4D–E). However, the vitality status of the trees had no significant effect on fungal  $\alpha$ -diversity (Table 2).

The vitality status of the trees altered prokaryotic and fungal  $\beta$ -diversity, explaining 8.1 % and 9.7 % of the variance (Table 2). Also, the drought legacy significantly affected  $\beta$ -diversity, explaining 19.9 % of the variability for prokaryotes and 8.1 % for fungi (Table 2). Each time point (vitality status) and drought legacy group combination harbored distinct microbial communities (Fig. 2). The CAP reclassification success rates – as a measure of the degree of discrimination between groups – decreased over time for prokaryotic communities, whereas the opposite pattern was observed for fungal communities (Fig. 2). Lower reclassification rates for the severe and intermediate drought legacy, especially at 'non-vital' and 'dead' status, indicated more minor differences in the prokaryotic community structures (Fig. 2A). Fungal community structure became more similar under the severe drought legacy; contrary to the other drought legacies, community structure became more distinct

at the vitality status 'dead' (Fig. 2B).

### 3.3. Trophic modes and taxa changing with the vitality status

Fourteen prokaryotic phyla and 1 fungal phylum significantly responded to the vitality status (PERMANOVA;  $q < 0.05$ ). A decrease in relative abundance under the vitality status 'non-vital' and 'dead' compared to the vitality status 'vital' was observed for the most responsive phyla (Fig. 3A). Only the phyla Verrucomicrobiota, Planctomycetota, and Chloroflexi increased in relative abundance toward the vitality status 'non-vital' and 'dead' (Fig. 3A).

The assignment of 1'175 fungal ASVs (40.0 % of the total fungal ASVs) to trophic modes revealed that saprotrophs dominated fungal communities (Fig. 3B). Saprotrophs had a significantly ( $P < 0.05$ ) lower mean relative abundance under the vitality status 'dead' than 'vital' (Fig. 3B). On the contrary, symbiotrophs significantly ( $P < 0.05$ ) increased in mean relative abundance under the vitality status 'non-vital' and 'dead' compared to the 'vital' status (Fig. 3B). However, no significant difference between the vitality status 'non-vital' and 'dead' was detected for any trophic mode. Pathotrophs did not significantly change in mean relative abundance between the vitality statuses (Fig. 3B).

After correction for multiple testing, 32 prokaryotic and 2 fungal genera with an overall abundance of  $>0.1$  % responded significantly to the vitality status (PERMANOVA;  $q < 0.05$ ). Cluster analysis showed

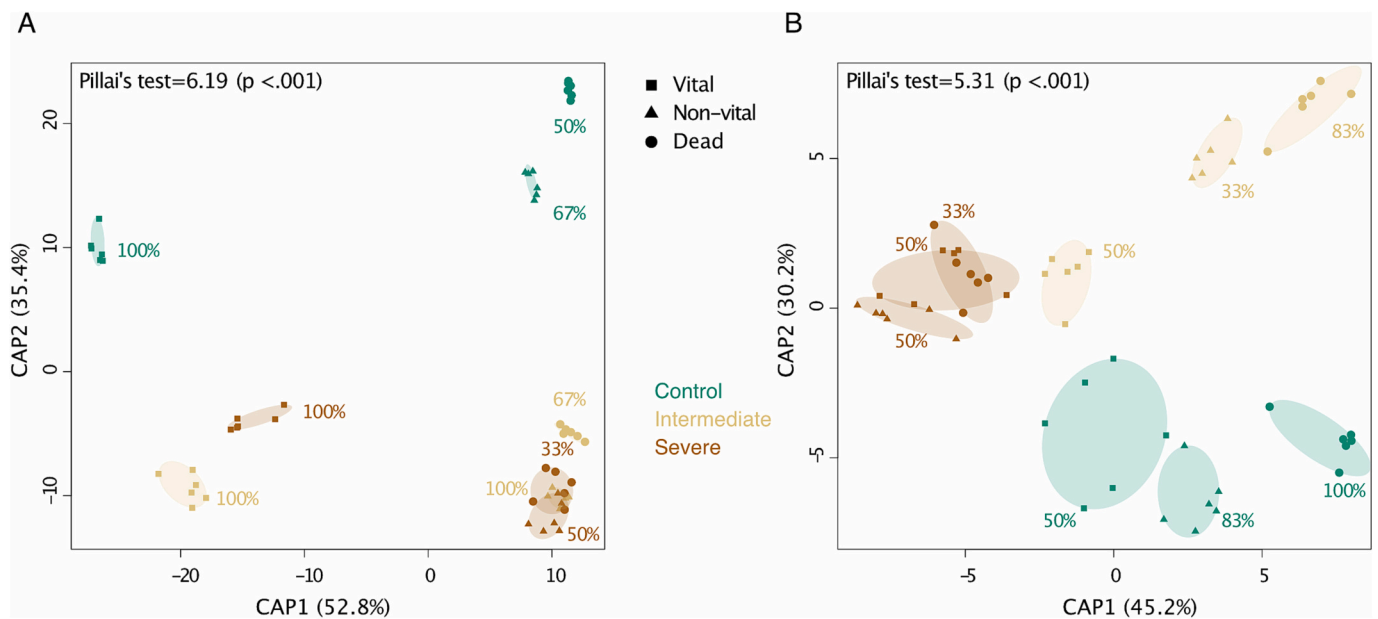


**Fig. 2.** Soil microbial community structures across drought legacies and vitality status. Canonical analysis of principal coordinates (CAP) constraining differences in prokaryotic (A) and fungal (B) community structure by drought legacy and vitality status. Axis CAP1 represents the effect of the vitality status, whereas axis CAP2 represents the drought legacy effect. The amount of between group variation of each CAP axis is provided in parenthesis. The CAP reclassification success rates provide a quantitative estimation of the degree of discrimination between the groups are provided next to each group. The CAP equivalent to Pillai's trace test (with  $P$ -value in brackets) indicating the overall effect size is provided at the top of the plot.

that these genera could be grouped into two main clusters (Fig. 4). Cluster I consisted of genera significantly increasing in relative abundance from 'vital' to 'non-vital' and from 'vital' to 'dead', respectively (Fig. 4). Genera in this cluster included members of the phyla Planctomycetota and Verrucomicrobiota and consisted of inter alia *Singulisphaera*, *Gemmata*, *Fimbrioglobus*, *Pirellula*, *Tundrisphaera*, and *Chthoniobacter*. Cluster II consisted of genera significantly decreasing in relative abundance from 'vital' to 'non-vital' and 'vital' to 'dead' (Fig. 4). Genera belonging to this cluster were widely spread across different phyla and included inter alia *Sphingomonas*, *Conexibacter*, *Haliangium*, *Mycobacterium*, *Bacillus*, *Hyphomicrobium*, *Pedomicrobium*, *Rhodomicrobium*. The fungal genera *Oidiodendron* and *Sagenomella* (Ascomycota) belonged to cluster II. The latter genus was the most abundant (8.15 %) and the only genus showing a significant change between 'non-vital' and 'dead' vitality status (Fig. 4).

### 3.4. Physicochemical soil properties

After the stop of the watering, the volumetric water content of the soils decreased significantly with time (vitality status of the trees,  $P < 0.001$ , Table 1), showing the most prominent reduction within the first 4 weeks (Supplementary Fig. 1A). However, soil volumetric water contents remained different among the three drought legacies ( $P < 0.001$ , Table 1) until the trees reached the vitality status 'non-vital' (~26 weeks after the stop of the watering). The VWC of control mesocosms and mesocosms previously treated with intermediate water limitation remained higher than those previously treated with severe water limitation (Supplementary Figs. 1A, 5A). Overall, VWC did not reach values below 5 % in any of the mesocosms (Supplementary Figs. 1A, 5A).

The vitality status of the trees significantly influenced all measured physicochemical soil properties, except for pH (Table 1). Soil organic carbon ( $C_{org}$ ), total carbon (TC), and total nitrogen (TN) concentrations increased from the vitality status 'vital' to 'non-vital' but decreased after the trees died (Supplementary Fig. 5C, 5D, 5E). However, the drought legacy did not appear to have a statistically significant effect. The soil C:N ratio differed significantly between the 'vital' status and the other states ( $P < 0.001$ , Table 1); after decreasing from the vitality status

'vital' to 'non-vital' and increasing toward the vitality status 'dead' in all drought legacies (Supplementary Fig. 5F). Soil ammonium ( $NH_4^+$ ) concentrations decreased after the trees reached the vitality status 'non-vital' (Supplementary Fig. 5G) and were significantly ( $P = 0.034$ , Table 1) lower under the vitality status 'dead' for all drought legacies. The opposite pattern was observed for soil nitrate ( $NO_3^-$ ) concentrations (Supplementary Fig. 5H), which increased toward the vitality status 'non-vital' ( $P < 0.001$ , Table 1) under all drought legacies and remained high at the vitality status 'dead'.

### 3.5. Relationship between microbial communities and tree or soil properties

There was a significant relationship between the composition of prokaryotic communities and soil VWC ( $P = 0.001$ ), tree height ( $P = 0.001$ ), and soil  $NO_3^-$  concentrations ( $P = 0.016$ ) (Supplementary Tables 1, 2). According to PERMANOVA and building a parsimonious model for parameter selection, VWC was the main driver among the measured physicochemical soil and plant properties. However, the db-RDA revealed that the effect of the VWC was mainly associated with the vitality status 'vital', and that the influence of the tree height was mainly associated with the control (Supplementary Fig. 6C). Fungal community composition was also significantly influenced by the VWC ( $P = 0.003$ ) (Supplementary Tables 1, 2).

## 4. Discussion

### 4.1. When trees die due to drought

In our study, the pace at which the trees died after the watering stop showed high variability among the trees, even those with the same drought history (Fig. 1D, Supplementary Fig. 1B). This variability, which was particularly marked for those trees that had been previously subjected to intermediate water limitation, highlights the individuality of the trees in terms of resistance to drought-induced tree mortality (Hartmann et al., 2018; Pretzsch et al., 2022). Since our study design had made sure to account for the potential differences in shading and



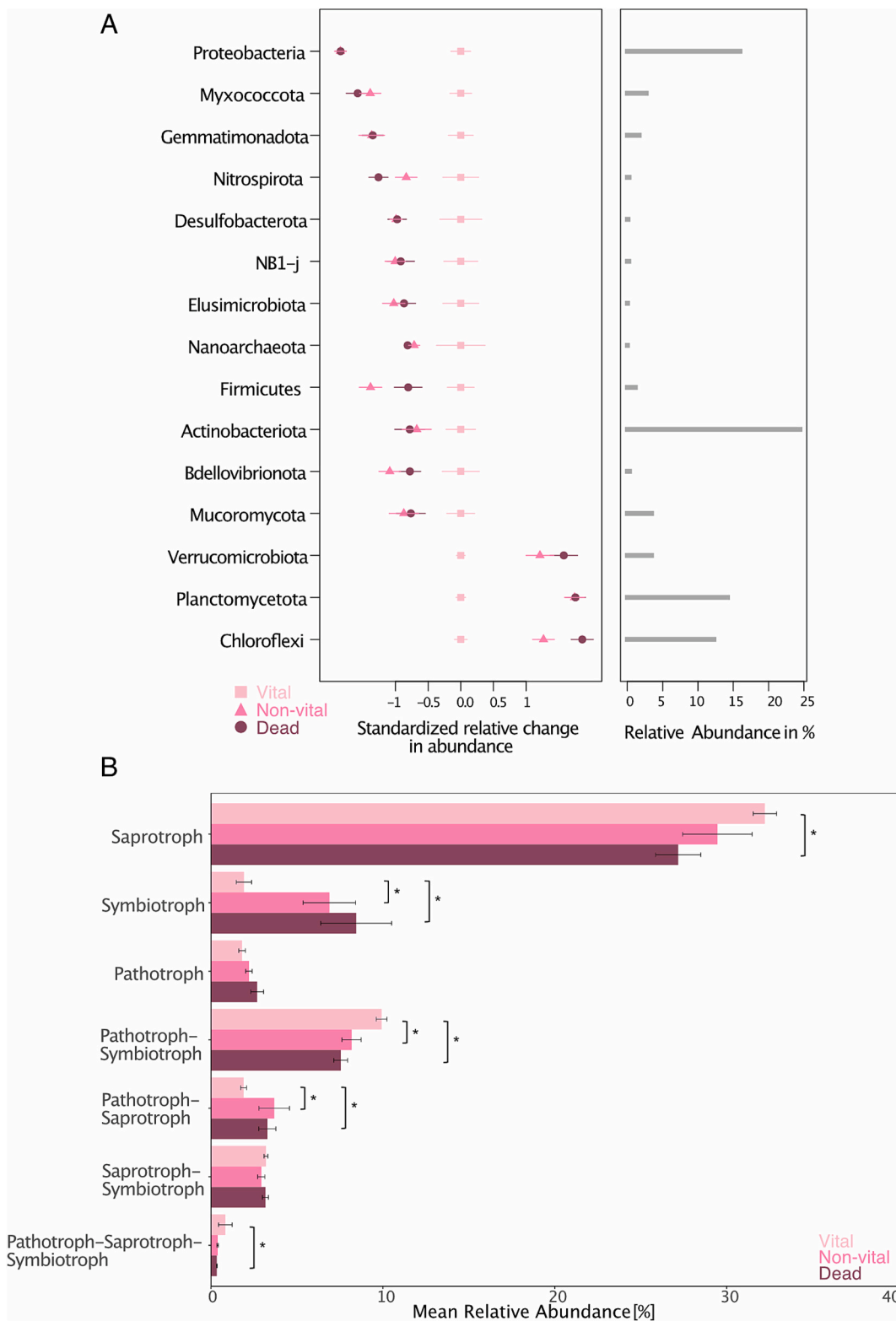


**Fig. 3.** Changes in the relative abundance of prokaryotic and fungal phyla, and fungal trophic modes under different tree vitality statuses. Relative change in abundance (z-transformed, to compare groups of different abundances) of fungal and prokaryotic phyla (A) under the ‘non-vital’ (=triangle) and ‘dead’ (=circle) vitality status compared to the ‘vital’ (=square) vitality status. The first vertical panel represents the standardized relative change in abundance from the mean, including the average change and the corresponding standard error (horizontal lines) — only phyla with significant ( $q < 0.05$ ) change in abundance are displayed. Change in mean relative abundance of fungal trophic modes under different tree vitality statuses (B). Trophic modes were assigned to ASVs with FUNGuild, and only classifications with ‘highly probable’ and ‘probable’ were displayed. Error bars represent the standard error of the mean. Significant differences ( $P < 0.05$ ) of pairwise comparisons are displayed with brackets and asterisk.

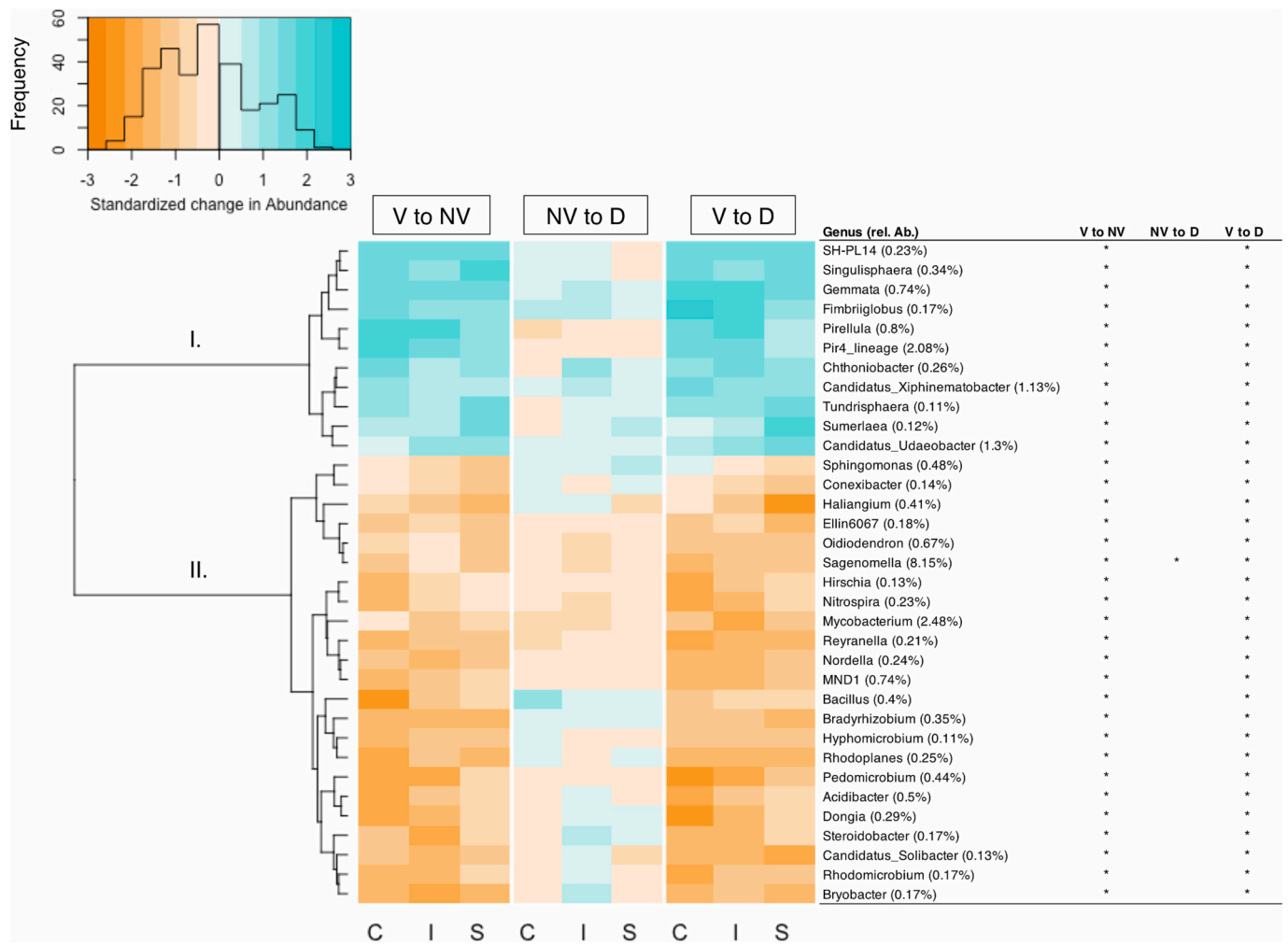


**Fig. 4.** Heatmap showing standardized changes in the relative abundance of genera between the different vitality statuses. Data were scaled (z-transformed) to compare groups of different abundances and only genera with a relative abundance  $>0.1$  % and a significant response to the status effect ( $q < 0.05$ ) are displayed. Changes in the relative abundance of genera between ‘vital’ to ‘non-vital’ (V to NV), from ‘non-vital’ to ‘dead’ (NV to D), and from ‘vital’ to ‘dead’ (V to D) were calculated for each drought legacy (C = control, I = Intermediate, S = Severe). Cluster analysis based on the Ward method was performed to group genera with similar response patterns. The two identified clusters corresponded to genera increasing in relative abundance (cluster I) and genera decreasing in relative abundance (cluster II). The overall relative abundance of each genus is provided in parenthesis after the name. Significant results ( $P < 0.05$ ) of pairwise comparisons between the statuses are indicated with an asterisk.

light availabilities in the greenhouse, the observed marked variability is likely not related to the position of the trees in the greenhouse but instead explained by a mesocosm-specific overlap between the spatial distribution of plant-resources and the acquisition-root system of the trees (Weemstra et al., 2016; Xia et al., 2010) or by plant-biotic interactions (Hartmann et al., 2018). Moreover, trees that survived longer might have emitted considerable amounts of below-ground volatile organic compounds (VOC) into the rhizosphere to defend against pathogenic microorganisms (Baetz and Martinoia, 2014).

Despite the high variability in the time needed for the trees to die in response to drought, we also observed some general trends. First, we observed a substantial decline in tree diameter (Table 1, Supplementary Fig. 2B). A shrinking of stem diameter as a reduction in basal area increment has been previously reported to be a phenomenon occurring during consecutive episodes of severe drought (Sánchez-Salguero et al., 2012) and is generally related to the tree water deficit (Güney et al., 2020). Secondly, we observed that needles turned dry and light green to brownish even before stomatal conductance decreased four weeks after the stop of the watering. This observation is linked to symptoms of plant water stress, as observed by Alizadeh et al. (2021).

Although we observed an early discoloration of the needles,

defoliation only started when soil VWC reached values below 10 %, indicating a threshold until which trees hold on to their needles. Tree defoliation was a reliable indication of a changing tree vitality status. Crown defoliation was shown to be a good predictor of tree mortality (Bussotti et al., 2021; de la Cruz et al., 2014; Dobbertin, 2005; Dobbertin and Brang, 2001; Eilmann et al., 2013) where trees pass a point of no return with defoliation levels of  $\geq 70$  % according to Hunziker et al. (2022).

The drought legacy of the mesocosms also appeared to shape the velocity at which the stomatal conductance declined in our study and, with it, the timing of the death of the trees (Supplementary Figs. 1B, 2D, Table 1). Drought legacies and the ability of trees to recover from previous drought events have already been identified as essential factors influencing the capacity of trees to resist or succumb to episodes of lack of available soil water (Galiano et al., 2011; Hartmann et al., 2018). For instance, the greater persistence of the trees in control mesocosm and in mesocosms with intermediate drought as compared to the trees which had been affected by severe drought (Fig. 1D, Supplementary Fig. 1B) could be related to the initial beneficial conditions for tree growth under more optimal soil water contents. These beneficial conditions might have resulted in comparatively better usage of non-structural

carbohydrates (NSC) necessary for osmoregulation and maintaining physiological functioning, which has been shown to support tree survival under drought (Gattmann et al., 2021; Sevanto et al., 2014).

The observed decrease in stomatal conductance (Supplementary Figs. 1, 2D) aligns with current knowledge that trees close their stomata under drought to reduce transpiration (Alizadeh et al., 2021). Reducing the stomatal gas exchange is an essential tree strategy to prevent hydraulic failure and carbon starvation (Chen et al., 2022). However, stomatal closure also reduces CO<sub>2</sub> diffusion into the leaf, hence C assimilation (Hartmann et al., 2018). It should be mentioned that the temperatures in the greenhouse in spring (as from week 20 after the stop of the watering) have potentially accelerated the process in which trees reached the 'non-vital' vitality status through higher evapotranspiration rates and soil water depletion (Supplementary Fig. 1). In the real world, a reduction of bioactive volatile organic compounds under increased temperatures, as observed by Rasheed et al. (2021), might further explain the quickened tree mortality under hot droughts (Allen et al., 2015). Moreover, increased susceptibility to pests and pathogens has been observed to lead to drought-induced tree mortality in many studies (e.g., Anderegg et al., 2015; Desprez-Loustau et al., 2006; Goodsman et al., 2013; Oliva et al., 2014; Xiong et al., 2011). However, since this mesocosm experiment was an artificial system without the introduction of biotic pests and herbivores, trees might have maintained resistance to death longer than in the field.

#### 4.2. Relationship between dying trees, soil properties, and soil microbial communities

The association between the aboveground biomass of the trees, measured as tree height, and prokaryotic communities (Supplementary Tables 1, 2, and Supplementary Fig. 6C) may point again to the individuality of trees and associated microbial communities. Thus, the extended survival of individual trees within the control may also relate to a microbially mediated drought tolerance (Allsup et al., 2023), for example, by ECM or diazotrophic bacteria.

The increase of NO<sub>3</sub><sup>-</sup> after the trees became 'non-vital' (Supplementary Fig. 5H) can be related to the fact that tree uptake of inorganic N diminished, and the activity of microbes with denitrification abilities was reduced as conditions in the soils became more oxic inhibiting denitrification as an anaerobic process (Edburg et al., 2012; Homyak et al., 2017). For example, the genus *Reyranella* (Proteobacteria), of which some species can reduce NO<sub>3</sub><sup>-</sup> (Kim et al., 2013; Lee et al., 2017), significantly decreased under the 'non-vital' and 'dead' vitality status compared to 'vital' (Fig. 4).

Total nitrogen (TN) concentrations in soils decreased after the trees reached a 'non-vital' vitality status (Supplementary Fig. 5D). At the same time, we found a decreased relative abundance of taxa known to be involved in N-fixation, which might explain the decrease in TN. For example, the diazotrophic genus *Bradyrhizobium* (Proteobacteria), involved in N fixation, decreased significantly from 'vital' to 'non-vital' (Fig. 4). Also, *Hyphomicrobium* (Proteobacteria) significantly decreased (Fig. 4), thus potentially limiting N availability through a reduction in N-fixation (Lladó et al., 2017; Oren and Xu, 2014).

The vitality status of the trees significantly influenced the soil microbiome (Fig. 2, Table 2). Nevertheless, significant changes in the soil microbiome at the genus level could only be detected from the tree status 'vital' to 'non-vital' and the tree status 'vital' to 'dead' in all drought legacies (Fig. 4). This shows that after the trees reached the vitality status of 'non-vital', there were no more significant effects on the genera composing the microbial communities, at least over the investigated time frame of 4 months. Furthermore, the drought legacy and vitality status interaction had no significant effect on microbial communities (Table 2). Nevertheless, the initial increase in soil nutrient pools and the absence of competition between trees and microbes for soil nutrients could also explain the observed changes in soil microbial communities independent of the drought history (Fig. 2).

#### 4.3. Changes of prokaryotic taxa during tree mortality

The increase of fungi when the trees became 'non-vital' (Supplementary Fig. 3B) might be explained by the fact that various fungal taxa could still access the remaining water in small soil pores through hyphal networks (Allen, 2007; Joergensen and Wichern, 2008). Moreover, trees might have maintained C allocation belowground, stimulating the abundance of beneficial fungal groups as ECM. Fungi might have been more sensitive at a later stage because they often reside in larger pores and on the surfaces of the aggregates, where they are more exposed to drying conditions (Denef et al., 2001; Six et al., 2006), and thus explains the strong effect of the decreasing VWC on soil fungi (Supplementary Tables 1, 2). Contrarily, bacteria might have instead been protected from desiccation in smaller soil pores and soil aggregates (Denef et al., 2001; Six et al., 2006), contributing to their increased abundance with drying. However, previous studies have shown that soil moisture at the sampling time is significantly related to the active part of the soil microbiome (Rajala et al., 2011), indicating that despite an increase in abundance, most bacteria in our system were potentially dormant (Blagodatskaya and Kuzyakov, 2013; Schimel et al., 2007).

Tree death increased prokaryotic diversity (except in mesocosms of the severe drought legacy) (Supplementary Fig. 4A–C). Tree death might have acted as a disturbance, promoting diversity by generating new habitats, increasing resource availability – through input of N-rich needle litter and organic C from dead roots while reducing plant N uptake – or releasing competition. We observed an increase in the relative abundance of oligotrophic phyla such as Planctomycetota, Verrucomicrobiota, and Chloroflexi (Fierer et al., 2007; Martens-Habbena et al., 2009; Trivedi et al., 2018) under tree death as we had expected (Fig. 3A). It is known that dry conditions can rapidly alter microbial communities toward oligotrophic groups, which can – compared to copiotrophic groups – survive with alternative types and availabilities of C resources (Aldén et al., 2001; Drenovsky et al., 2004; Soong et al., 2020), an advantage that might explain the observed decrease of TC concentrations in the soils (Supplementary Fig. 5D). A previous study in the same mesocosm system already showed a switch from copiotrophic to oligotrophic lifestyles in prokaryotic communities under prolonged water limitation (Jaeger et al., 2023b, in press). At the same time, this might also point to a slowdown of the C turnover rate.

Planctomycetota are widely distributed in terrestrial environments and across diverse environmental and physicochemical conditions, which suggests a broad capacity to adapt to diverse harsh environmental conditions (Kaboré et al., 2020). Most genera of the phylum Planctomycetota are aerobic chemoorganotrophs and chemoheterotrophs (Rosenberg et al., 2014). Additionally, Planctomycetota are characterized as oligotrophic and slow-growing (Fuerst, 2017) and were shown to increase under oligotrophic conditions in a Scots pine forest (Hartmann et al., 2017). The genera *SH-PL14*, *Singulisphaera*, *Gemmata*, *Fimbriglobus*, *Pirellula*, *Pir4\_lineage*, and *Tundrisphaera* significantly increased from the vitality status 'vital' to 'non-vital' and 'dead' in all drought legacies (Fig. 4, cluster I). These genera are highly abundant in peatlands and forested tundra soil, where they appear to play an essential role in decomposing Sphagnum-derived litter (Ivanova et al., 2016; Kulichevskaya et al., 2007). The genus *Gemmata* was also detected to be highly abundant under drought (Bouskill et al., 2013; Tóth et al., 2017). Ultimately, some species of the Planctomycetota are capable of ammonia oxidation in an anaerobic double membrane (anammoxosome) (Fuerst and Sagulenko, 2011; van Niftrik and Jetten, 2012), and the observed increase of Planctomycetota could have contributed to the observed decrease of NH<sub>4</sub><sup>+</sup> and increase of NO<sub>3</sub><sup>-</sup> in our study (Supplementary Fig. 5G, 5H). An increase in nitrification under dry and thus more aerobic conditions has also been reported in a study by Parker and Schimel (2011) in Mediterranean climate California grasslands and by Homyak et al. (2014) in a dry watershed ecosystem. Ecologically increased NH<sub>4</sub><sup>+</sup> oxidation can lead to increased levels of N<sub>2</sub> respired back into the atmosphere, and increased NO<sub>3</sub><sup>-</sup> concentrations without plant

uptake can enhance the risk of rapid N losses from the soil system, i.e., through leaching.

#### 4.4. The role of fungal saprotrophs and symbiotrophs

Although we had expected to find an associated increase in saprotrophic fungi, tree death had contrasting impacts on fungal trophic modes, and saprotrophs did not increase (Fig. 3B) but significantly decreased from the vitality status 'vital' to 'dead'. For example, the most abundant taxon in our soils, the saprotrophic genus *Sagenomella* (Ascomycota), was significantly affected by the trees' vitality status, decreasing in relative abundance when the vitality status changed to 'dead' (Fig. 4). Also, *Oidiiodendron*, identified as a decomposer of forest litter in a study by Štursová et al. (2012), significantly decreased in our system during tree death (Fig. 4). However, *Oidiiodendron* spp. are root-associated (Clemmensen et al., 2015), which could explain their decrease when the host tree died. Saprotrophs predominantly colonize recently fallen cellulose-rich litter components closer to the surface (Lindahl et al., 2007). Nonetheless, it has been shown that under conditions of nutrient limitation, saprotrophic microbes prefer microbially processed organic matter (OM) with a lower C:N ratio and thereby mine persistent soil organic matter (SOM) rather than plant-derived OM (Hicks et al., 2021). SOM might have been easier to access than lignin from dead plant material, explaining the reduced  $C_{org}$  concentrations in the soil (Supplementary Fig. 3C), which points to potential C losses. Moreover, the decomposition of SOM is mainly dependent on soil moisture (Tóth et al., 2017); therefore, the dry soil conditions during the experiment may have potentially inhibited saprotrophic activities.

Although we had expected that symbiotrophs, such as ECM, would significantly decrease after tree death because of their close association with the host, we observed the opposite. Symbiotrophs significantly increased from 'vital' to 'non-vital' and from 'vital' to 'dead' (Fig. 3B). ASVs increasing under tree death belonged to the phyla Ascomycota and Basidiomycota (Tedersoo et al., 2010; Voriskova and Baldrian, 2013) and were assigned as the fungal guild ECM. ECM have been suggested to play an active role in decomposition processes (Rajala et al., 2011) and thus may act as facultative saprotrophs (Lindahl and Tunlid, 2015), which could explain their increased abundance under tree death. Recent studies found that ECM fungi have significant capacities to assimilate organic N associated with SOM and mineral surfaces, reflecting the capacity of lignocellulose decomposition (Frey, 2019; Tunlid et al., 2022; Zak et al., 2019). Moreover, certain groups of ECM are suggested to be actively decomposing C while they mine SOM for N and complement free-living decomposers (Argiroff et al., 2022; Lindahl et al., 2021; Mayer et al., 2023; Shao et al., 2023), which could further explain their increased abundance with tree mortality. In turn, free-living saprotrophic microbes (fungal and prokaryotic) compete for the same resources as ECM fungi (Fernandez and Kennedy, 2016; Mayer et al., 2023). Also, the increase of symbiotrophs could be linked to the observed increase in the relative abundance of fungi under the 'non-vital' status (Supplementary Fig. 3B) and might reflect a survival strategy of the trees. To survive under extreme drought stress, trees potentially supplied C belowground to maintain the interchange with ECM (Usman et al., 2021), increasing the abundance of symbiotrophs during tree death. Alternatively, the increase of symbiotrophs could result from increased spore production of ECM, forming a soil spore bank (Glassman et al., 2016; Nara, 2009) to endure unfavorable conditions when the host dies and enable quick colonization after re-establishing of seedlings (Baar et al., 1999).

In any case, it should be mentioned that although we could detect changes in the composition of fungal trophic modes in our study, only 40 % of the fungal ASVs could be assigned to fungal guilds, and proportions might not reflect actual abundances. Moreover, the observation time of four months from 'non-vital' to 'dead' might have been too short for detecting classical succession patterns, especially of groups involved in decomposing dead plant material.

#### 4.5. Legacy effect of the drought treatments

The drought legacy of the mesocosms significantly affected  $\beta$ -diversity (Table 2), pointing to an effect of the drought history of the soils as we had hypothesized. The strong effect of the previous water limitation treatment is potentially related to the differing VWC when the trees were still 'vital' and the subsequent decrease during the following weeks, where the soil of the mesocosms that had been treated with severe water limitation dried out faster (Supplementary Figs. 1A, 5A). It is known that extreme drought may imprint a legacy signature in the soil microbiome composition that can last for weeks after the end of a drought event; however, until now, these effects have been mainly studied in drying and rewetting events (e.g., Barnard et al., 2013; Fuchslueger et al., 2016; Meisner et al., 2018). We found no interaction between the effects of drought legacy and vitality status (Table 2). As a result, the difference in the community structure between the drought legacies remained comparable among the vitality status of the trees (Fig. 2). However, the structure of microbial communities in the intermediate and severe drought legacies was more similar compared to that of the control. This similarity relates to a similar drought history of microbial communities exposed to severe and intermediate water limitations in our study (Fig. 2). In contrast, the community structure in mesocosms of the control became more distinct at the vitality status 'dead' (Fig. 2).

We did not observe significant changes in fungal trophic modes and on the genus level between the 'non-vital' and 'dead' vitality status (Figs. 3, 4), so the composition of microbial communities associated with trees in these stages was more similar than that of vital trees (Fig. 2), especially in the severe drought legacy. We relate this observation to the fact that water, essential for microbial processes (Tecon and Or, 2017; Vos et al., 2013), was missing at those stages to introduce more significant changes in the community structure during tree mortality.

## 5. Conclusion

Our study reveals that tree mortality is influenced by drought history but that the phase of dying in an artificial system could take longer than in nature due to a lack of pests and pathogens. Furthermore, our results show that tree death is highly variable within drought legacies, pointing to the individuality of trees. The presented results indicate that signs of tree mortality associated with water stress are next to a decrease in stomatal conductance, a discoloring of needles, increased defoliation, and a shrinkage of the stem diameter. We could show that soil  $NO_3^-$  concentrations increase after tree death probably through diminished plant uptake and potentially increased microbial nitrification activity. Our findings reveal that tree death and drought legacy affect microbial abundance and community compositions. Specifically, we could show that copiotrophic bacterial taxa decrease during tree mortality while oligotrophic increase, which could slow soil C turnover. Furthermore, our results indicate that fungal saprotrophs decrease while symbiotrophs increase in abundance during tree mortality. This could be related to the ability of ECM to be facultative saprotrophic or the increased spore production of ECM when the host dies. Moreover, an increased C supply to symbiotrophs could reflect a survival strategy of trees. Overall, the presented findings contribute to our understanding of how changes in prokaryotic and fungal communities following drought-induced tree death might affect soil processes in forest ecosystems.

## Funding statement

This work was supported by the Swiss National Science Foundation (SNSF, Ambizione grant number PZ00P2\_180030) granted to EFS.

## CRediT authorship contribution statement

**Astrid C.H. Jaeger:** Data curation, Formal analysis, Conceptualization, Investigation, Methodology, Software, Visualization, Writing – original draft, Writing – review & editing. **Martin Hartmann:** Data curation, Formal analysis, Conceptualization, Methodology, Software, Visualization, Supervision, Writing – review & editing. **Rafaela Feola Gonz:** Investigation, Methodology, Writing – review & editing. **Johan Six:** Resources, Conceptualization, Supervision, Writing – review & editing. **Emily F. Solly:** Funding acquisition, Conceptualization, Methodology, Investigation, Project administration, Supervision, Writing – review & editing.

## Declaration of competing interest

The authors declare that they have no known competing financial interests or personal relationships that could have appeared to influence the work reported in this paper.

## Data availability

The sequence data of this study have been submitted to the European Nucleotide Archive (ENA) at EMBL-EBI (<http://www.ebi.ac.uk/>) under accession numbers PRJEB61158 and PRJEB64205. Metadata supporting this study's findings is available from the corresponding author upon reasonable request.

## Acknowledgments

We thank the members of the ETH research station for plant sciences in Lindau for using their equipment and facilities. We particularly thank Matti Barthel, Brigitta Herzog, and Britta Jahn-Humphrey for their technical support in the greenhouse and laboratory. We further acknowledge the help of Louise Humbert and Charles Nwokoro with analyses in the laboratory. We also thank Maria Domenica Moccia at the Functional Genomics Center Zurich (FGCZ) for providing the sequencing service on the Illumina MiSeq platform. The graphical abstract was created using [BioRender.com](https://BioRender.com).

## Appendix A. Supplementary data

Supplementary data to this article can be found online at <https://doi.org/10.1016/j.apsoil.2023.105198>.

## References

- Abarenkov, K., Henrik Nilsson, R., Larsson, K.-H., Alexander, L.J., Eberhardt, U., Erland, S., Høiland, K., Kjeller, R., Larsson, E., Pennanen, T., Sen, R., Taylor, A.F.S., Tederso, L., Ursing, B.M., Vrålstad, T., Liimatainen, K., Peintner, U., Kõljalg, U., 2010. The UNITE database for molecular identification of fungi – recent updates and future perspectives. *New Phytol.* 186, 281–285. <https://doi.org/10.1111/j.1469-8137.2009.03160.x>.
- Adams, H.D., Germino, M.J., Breshears, D.D., Barron-Gafford, G.A., Guardiola-Claramonte, M., Zou, C.B., Huxman, T.E., 2013. Nonstructural leaf carbohydrate dynamics of *Pinus edulis* during drought-induced tree mortality reveal role for carbon metabolism in mortality mechanism. *New Phytol.* 197, 1142–1151. <https://doi.org/10.1111/nph.12102>.
- Adams, H.D., Barron-Gafford, G.A., Minor, R.L., Gardea, A.A., Bentley, L.P., Law, D.J., Breshears, D.D., McDowell, N.G., Huxman, T.E., 2017a. Temperature response surfaces for mortality risk of tree species with future drought. *Environ. Res. Lett.* 12. <https://doi.org/10.1088/1748-9326/aa93be>.
- Adams, H.D., Zeppel, M.J.B., Anderegg, W.R.L., Hartmann, H., Landhäusser, S.M., Tissue, D.T., Huxman, T.E., Hudson, P.J., Franz, T.E., Allen, C.D., Anderegg, L.D.L., Barron-Gafford, G.A., Beerling, D.J., Breshears, D.D., Brodrribb, T.J., Bugmann, H., Cobb, R.C., Collins, A.D., Dickman, L.T., Duan, H., Ewers, B.E., Galiano, L., Galvez, D.A., Garcia-Forner, N., Gaylord, M.L., Germino, M.J., Gessler, A., Hacke, U. G., Hakamada, R., Hector, A., Jenkins, M.W., Kane, J.M., Kolb, T.E., Law, D.J., Lewis, J.D., Limousin, J.M., Love, D.M., Macalady, A.K., Martínez-Vilalta, J., Mencuccini, M., Mitchell, P.J., Muss, J.D., O'Brien, M.J., O'Grady, A.P., Pangle, R.E., Pinkard, E.A., Piper, F.I., Plaut, J.A., Pockman, W.T., Quirk, J., Reinhardt, K., Ripullone, F., Ryan, M.G., Sala, A., Sevanto, S., Sperry, J.S., Vargas, R., Vennetier, M., Way, D.A., Xu, C., Yepez, E.A., McDowell, N.G., 2017b. A multi-species synthesis of physiological mechanisms in drought-induced tree mortality. *Nat. Ecol. Evol.* 1, 1285–1291. <https://doi.org/10.1038/s41559-017-0248-x>.
- Aldén, L., Demoling, F., Bååth, E., 2001. Rapid method of determining factors limiting bacterial growth in soil. *Appl. Environ. Microbiol.* 67, 1830–1838. <https://doi.org/10.1128/AEM.67.4.1830-1838.2001>.
- Alizadeh, A., Toudeshki, A., Ehsani, R., Migliacchi, K., Wang, D., 2021. Detecting tree water stress using a trunk relative water content measurement sensor. *Smart Agric. Technol.* 1, 100003. <https://doi.org/10.1016/j.atech.2021.100003>.
- Allen, M.F., 2007. Mycorrhizal fungi: highways for water and nutrients in arid soils. *Vadose Zo. J.* 6, 291–297. <https://doi.org/10.2136/vzj2006.0068>.
- Allen, C., Macalady, A.K., Chenchouni, H., Bachelet, D., McDowell, N., Vennetier, M., Kitzberger, T., Rigling, A., Breshears, D.D., Hogg, E.H. (Ted), Gonzalez, P., Fensham, R., Zhang, Z., Castro, J., Demidova, N., Lim, J.-H., Allard, G., Running, S. W., Semerci, A., Cobb, N., 2010. A global overview of drought and heat-induced tree mortality reveals emerging climate change risks for forests. *For. Ecol. Manage.* 259, 660–684. <https://doi.org/10.1016/j.foreco.2009.09.001>.
- Allen, C., Breshears, D.D., McDowell, N.G., 2015. On underestimation of global vulnerability to tree mortality and forest die-off from hotter drought in the Anthropocene. *Ecosphere* 6, 1–55. <https://doi.org/10.1890/ES15-00203.1>.
- Allsup, C.M., George, L., Lankau, R.A., 2023. Shifting microbial communities can enhance tree tolerance to changing climates. *Science* (80-) 380, 835–840. <https://doi.org/10.1126/science.adf2027>.
- Anderegg, W.R.L., Kane, J.M., Anderegg, L.D.L., 2013. Consequences of widespread tree mortality triggered by drought and temperature stress. *Nat. Clim. Chang.* 3, 30–36. <https://doi.org/10.1038/nclimate1635>.
- Anderegg, W.R.L., Hicke, J.A., Fisher, R.A., Allen, C.D., Aukema, J., Bentz, B., Hood, S., Lichstein, J.W., Macalady, A.K., McDowell, N., Pan, Y., Raffa, K., Sala, A., Shaw, J. D., Stephenson, N.L., Tague, C., Zeppel, M., 2015. Tree mortality from drought, insects, and their interactions in a changing climate. *New Phytol.* 208, 674–683. <https://doi.org/10.1111/nph.13477>.
- Anderegg, W.R.L., Martínez-Vilalta, J., Cailleret, M., Camarero, J.J., Ewers, B.E., Galbraith, D., Gessler, A., Grote, R., Huang, C.Ying., Levick, S.R., Powell, T.L., Rowland, L., Sánchez-Salguero, R., Trotsiuk, V., 2016. When a tree dies in the forest: scaling climate-driven tree mortality to ecosystem water and carbon fluxes. *Ecosystems* 19, 1133–1147. <https://doi.org/10.1007/s10021-016-9982-1>.
- Anderson, M.J., 2001. A new method for non-parametric multivariate analysis of variance. *Austral Ecol.* 26, 32–46. <https://doi.org/10.1046/j.1442-9993.2001.01070.x>.
- Anderson, M.J., 2006. Distance-based tests for homogeneity of multivariate dispersions. *Biometrics* 62, 245–253. <https://doi.org/10.1111/j.1541-0420.2005.00440.x>.
- Anderson, M.J., Willis, T.J., 2003. Canonical analysis of principal coordinates: a useful method of constrained ordination for ecology. *Ecology* 84, 511–525. [https://doi.org/10.1890/0012-9658\(2003\)084\[0511:CAOPCA\]2.0.CO;2](https://doi.org/10.1890/0012-9658(2003)084[0511:CAOPCA]2.0.CO;2).
- Argiroff, W.A., Zak, D.R., Pellitier, P.T., Upchurch, R.A., Belke, J.P., 2022. Decay by ectomycorrhizal fungi couples soil organic matter to nitrogen availability. *Ecol. Lett.* 25, 391–404. <https://doi.org/10.1111/ele.13923>.
- Avila, J.M., Gallardo, A., Ibáñez, B., Gómez-Aparicio, L., 2016. *Quercus suber* dieback alters soil respiration and nutrient availability in Mediterranean forests. *J. Ecol.* 104, 1441–1452. <https://doi.org/10.1111/1365-2745.12618>.
- Ávila, J.M., Gallardo, A., Ibáñez, B., Gómez-Aparicio, L., 2021. Pathogen-induced tree mortality modifies key components of the C and N cycles with no changes on microbial functional diversity. *Ecosystems* 24, 451–466. <https://doi.org/10.1007/s10021-020-00528-1>.
- Baar, J., Horton, T.R., Kretzer, A., Bruns, T.D., 1999. From resistant propagules after a stand-replacing wildfire. *New Phytol.* 143, 409–418. <https://doi.org/10.1046/j.1469-8137.1999.00452.x>.
- Baetz, U., Martiñoia, E., 2014. Root exudates: the hidden part of plant defense. *Trends Plant Sci.* 19, 90–98. <https://doi.org/10.1016/j.tplants.2013.11.006>.
- Baldrian, P., López-Mondéjar, R., Kohout, P., 2023. Forest microbiome and global change. *Nat. Rev. Microbiol.* <https://doi.org/10.1038/s41579-023-00876-4>.
- Barnard, R.L., Osborne, C.A., Firestone, M.K., 2013. Responses of soil bacterial and fungal communities to extreme desiccation and rewetting. *ISME J.* 7, 2229–2241. <https://doi.org/10.1038/ismej.2013.104>.
- Bengtsson-Palme, J., Ryberg, M., Hartmann, M., Branco, S., Wang, Z., Godhe, A., De Wit, P., Sánchez-García, M., Ebersberger, I., de Sousa, F., Amend, A., Jumpponen, A., Unterseher, M., Kristiansson, E., Abarenkov, K., Bertrand, Y.J.K., Sanli, K., Eriksson, K.M., Vik, U., Veldre, V., Nilsson, R.H., 2013. Improved software detection and extraction of ITS1 and ITS2 from ribosomal ITS sequences of fungi and other eukaryotes for analysis of environmental sequencing data. *Methods Ecol. Evol.* 4, 914–919. <https://doi.org/10.1111/2041-210X.12073>.
- Bengtsson-Palme, J., Hartmann, M., Eriksson, K.M., Pal, C., Thorell, K., Larsson, D.G.J., Nilsson, R.H., 2015. metaxa2: improved identification and taxonomic classification of small and large subunit rRNA in metagenomic data. *Mol. Ecol. Resour.* 15, 1403–1414. <https://doi.org/10.1111/1755-0998.12399>.
- Blagodatskaya, E., Kuzyakov, Y., 2013. Active microorganisms in soil: critical review of estimation criteria and approaches. *Soil Biol. Biochem.* 67, 192–211. <https://doi.org/10.1016/j.soilbio.2013.08.024>.
- Bouskill, N.J., Lim, H.C., Borghin, S., Salve, R., Wood, T.E., Silver, W.L., Brodie, E.L., 2013. Pre-exposure to drought increases the resistance of tropical forest soil bacterial communities to extended drought. *ISME J.* 7, 384–394. <https://doi.org/10.1038/ismej.2012.113>.
- Bussotti, F., Papitto, G., Di Martino, D., Cocciufa, C., Cindolo, C., Cenni, E., Bettini, D., Iacopetti, G., Pollastrini, M., 2021. Defoliation, recovery and increasing mortality in Italian forests: levels, patterns and possible consequences for forest multifunctionality. *Forests* 12, 1–12. <https://doi.org/10.3390/f12111476>.

- Carnicer, J., Coll, M., Ninyerola, M., Pons, X., Sánchez, G., Peñuelas, J., 2011. Widespread crown condition decline, food web disruption, and amplified tree mortality with increased climate change-type drought. *Proc. Natl. Acad. Sci.* 108, 1474–1478. <https://doi.org/10.1073/pnas.1010070108>.
- Chen, Z., Li, S., Wan, X., Liu, S., 2022. Strategies of tree species to adapt to drought from leaf stomatal regulation and stem embolism resistance to root properties. *Front. Plant Sci.* 13, 1–18. <https://doi.org/10.3389/fpls.2022.926535>.
- Cigan, P.W., Karst, J., Cahill, J.F., Sywenky, A.N., Pec, G.J., Erbilgin, N., 2015. Influence of bark beetle outbreaks on nutrient cycling in native pine stands in western Canada. *Plant and Soil* 390, 29–47. <https://doi.org/10.1007/s11104-014-2378-0>.
- Clemmensen, K.E., Finlay, R.D., Dahlberg, A., Stenlid, J., Wardle, D.A., Lindahl, B.D., 2015. Carbon sequestration is related to mycorrhizal fungal community shifts during long-term succession in boreal forests. *New Phytol.* 205, 1525–1536. <https://doi.org/10.1111/nph.13208>.
- Custer, G.F., van Diepen, L.T.A., Stump, W.L., 2020. Structural and functional dynamics of soil microbes following spruce beetle infestation. *Appl. Environ. Microbiol.* 86, 1–14. <https://doi.org/10.1128/AEM.01984-19>.
- de la Cruz, A.C., Gil, P.M., Fernández-Cancio, Á., Minaya, M., Navarro-Cerrillo, R.M., Sánchez-Salguero, R., Grau, J.M., 2014. Defoliation triggered by climate induced effects in Spanish ICP forests monitoring plots. *For. Ecol. Manage.* 331, 245–255. <https://doi.org/10.1016/j.foreco.2014.08.010>.
- Denef, K., Six, J., Bossuyt, H., Frey, S.D., Elliott, E.T., Merckx, R., Paustian, K., 2001. Influence of dry-wet cycles on the interrelationship between aggregate, particulate organic matter, and microbial community dynamics. *Soil Biol. Biochem.* 33, 1599–1611. [https://doi.org/10.1016/S0038-0717\(01\)00076-1](https://doi.org/10.1016/S0038-0717(01)00076-1).
- Desprez-Loustau, M.-L., Marçais, B., Nagelisen, L.-M., Piou, D., Vannini, A., 2006. Interactive effects of drought and pathogens in forest trees. *Ann. For. Sci.* 63, 597–612. <https://doi.org/10.1051/forest:2006040>.
- Doane, T.A., Horwath, W.R., 2003. Spectrophotometric determination of nitrate with a single reagent. *Anal. Lett.* 36, 2713–2722. <https://doi.org/10.1081/AL-120024647>.
- Dobbertin, M., 2005. Tree growth as indicator of tree vitality and of tree reaction to environmental stress: a review. *Eur. J. For. Res.* 124, 319–333. <https://doi.org/10.1007/s10342-005-0085-3>.
- Dobbertin, M., Brang, P., 2001. Crown defoliation improves tree mortality models. *For. Ecol. Manage.* 141, 271–284. [https://doi.org/10.1016/S0378-1127\(00\)00335-2](https://doi.org/10.1016/S0378-1127(00)00335-2).
- Dobbertin, M., Hug, C., Mizoue, N., 2004. Using slides to test for changes in crown defoliation assessment methods. Part I: visual assessment of slides. *Environ. Monit. Assess.* 98, 295–306. <https://doi.org/10.1023/B:EMAS.0000038192.84631.b6>.
- Drenovsky, R.E., Vo, D., Graham, K.J., Scow, K.M., 2004. Soil water content and organic carbon availability are major determinants of soil microbial community composition. *Microb. Ecol.* 48, 424–430. <https://doi.org/10.1007/s00248-003-1063-2>.
- Edburg, S.L., Hicke, J.A., Brooks, P.D., Pendall, E.G., Ewers, B.E., Norton, U., Gochis, D., Gutmann, E.D., Meddens, A.J., 2012. Cascading impacts of bark beetle-caused tree mortality on coupled biogeophysical and biogeochemical processes. *Front. Ecol. Environ.* 10, 416–424. <https://doi.org/10.1890/110173>.
- Edgar, R., 2016a. UNOISE2: Improved Error-correction for Illumina 16S and ITS Amplicon Sequencing. *bioRxiv* 081257. <https://doi.org/10.1101/081257>.
- Edgar, R., 2016b. SINTAX: A Simple non-Bayesian Taxonomy Classifier for 16S and ITS Sequences. *bioRxiv* 074161. <https://doi.org/10.1101/074161>.
- Edgar, R.C., 2016c. UCHIME2: Improved Chimera Prediction for Amplicon Sequencing. *bioRxiv* 074252. <https://doi.org/10.1101/074252>.
- Edgar, R.C., Flyvbjerg, H., 2015. Error filtering, pair assembly and error correction for next-generation sequencing reads. *Bioinformatics* 31, 3476–3482. <https://doi.org/10.1093/bioinformatics/btv401>.
- Eilmann, B., Dobbertin, M., Rigling, A., 2013. Growth response of Scots pine with different crown transparency status to drought release. *Ann. For. Sci.* 70, 685–693. <https://doi.org/10.1007/s13595-013-0310-z>.
- Etzold, S., Ziemińska, K., Rohner, B., Bottero, A., Bose, A.K., Ruehr, N.K., Zingg, A., Rigling, A., 2019. One century of forest monitoring data in Switzerland reveals species- and site-specific trends of climate-induced tree mortality. *Front. Plant Sci.* 10, 1–18. <https://doi.org/10.3389/fpls.2019.00307>.
- Fernandez, C.W., Kennedy, P.G., 2016. Revisiting the “Gadgil effect”: do interguild fungal interactions control carbon cycling in forest soils? *New Phytol.* 209, 1382–1394. <https://doi.org/10.1111/nph.13648>.
- Fierer, N., Bradford, M.A., Jackson, R.B., 2007. Toward an ecological classification of soil bacteria. *Ecology* 88, 1354–1364. <https://doi.org/10.1890/05-1839>.
- Fontaine, S., Barot, S., Barré, P., Bdioui, N., Mary, B., Rumpel, C., 2007. Stability of organic carbon in deep soil layers controlled by fresh carbon supply. *Nature* 450, 277–280. <https://doi.org/10.1038/nature06275>.
- Forster, J.C., 1995. Soil sampling, handling, storage and analysis. In: *Methods in Applied Soil Microbiology and Biochemistry*. <https://doi.org/10.1016/b978-012513840-6/50018-5>.
- Franklin, J.F., Shugart, H.H., Harmon, M.E., 1987. Tree death as an ecological process. *Bioscience* 37, 550–556. <https://doi.org/10.2307/1310665>.
- Frey, S.D., 2019. Mycorrhizal fungi as mediators of soil organic matter dynamics. *Annu. Rev. Ecol. Syst.* 50, 237–259. <https://doi.org/10.1146/annurev-ecolsys-110617-062331>.
- Frey, B., Rime, T., Phillips, M., Stierli, B., Hajdas, I., Widmer, F., Hartmann, M., 2016. Microbial diversity in European alpine permafrost and active layers. *FEMS Microbiol. Ecol.* 92, 1–17. <https://doi.org/10.1093/femsec/fiw018>.
- Fuchslueger, L., Bahn, M., Hasibeder, R., Kienzl, S., Fritz, K., Schmitt, M., Watzka, M., Richter, A., 2016. Drought history affects grassland plant and microbial carbon turnover during and after a subsequent drought event. *J. Ecol.* 104, 1453–1465. <https://doi.org/10.1111/1365-2745.12593>.
- Fuerst, J.A., 2017. *Planctomycetes — New Models for Microbial Cells and Activities, Microbial Resources*. Elsevier Inc. <https://doi.org/10.1016/B978-0-12-804765-1/00001-1>.
- Fuerst, J.A., Sagulenko, E., 2011. Beyond the bacterium: planctomycetes challenge our concepts of microbial structure and function. *Nat. Rev. Microbiol.* 9, 403–413. <https://doi.org/10.1038/nrmicro2578>.
- Galiano, L., Martínez-Vilalta, J., Lloret, F., 2011. Carbon reserves and canopy defoliation determine the recovery of Scots pine 4yr after a drought episode. *New Phytol.* 190, 750–759. <https://doi.org/10.1111/j.1469-8137.2010.03628.x>.
- Gattmann, M., Birami, B., Nadal Sala, D., Ruehr, N.K., 2021. Dying by drying: timing of physiological stress thresholds related to tree death is not significantly altered by highly elevated CO<sub>2</sub>. *Plant Cell Environ.* 44, 356–370. <https://doi.org/10.1111/pce.13937>.
- Glassman, S.I., Levine, C.R., Dirocco, A.M., Battles, J.J., Bruns, T.D., 2016. Ectomycorrhizal fungal spore bank recovery after a severe forest fire: some like it hot. *ISME J.* 10, 1228–1239. <https://doi.org/10.1038/ismej.2015.182>.
- Gómez-Aparicio, L., Domínguez-Begines, J., Villa-Sanabria, E., García, L.V., Muñoz-Pajares, A.J., 2022. Tree decline and mortality following pathogen invasion alters the diversity, composition and network structure of the soil microbiome. *Soil Biol. Biochem.* 166. <https://doi.org/10.1016/j.soilbio.2022.108560>.
- Goodman, D.W., Lusebrink, I., Landhüsser, S.M., Erbilgin, N., Lieffers, V.J., 2013. Variation in carbon availability, defence chemistry and susceptibility to fungal invasion along the stems of mature trees. *New Phytol.* 197, 586–594. <https://doi.org/10.1111/nph.12019>.
- Göransson, H., Godbold, D.L., Jones, D.L., Rousk, J., 2013. Bacterial growth and respiration responses upon rewetting dry forest soils: impact of drought-legacy. *Soil Biol. Biochem.* 57, 477–486. <https://doi.org/10.1016/j.soilbio.2012.08.031>.
- Gower, J.C., 2015. *Principal Coordinates Analysis*. Wiley StatsRef Stat. Ref. Online, pp. 1–7. <https://doi.org/10.1002/9781118445112.stat05670.pub2>.
- Güney, A., Zweifel, R., Türkan, S., Zimmermann, R., Wachendorf, M., Güney, C.O., 2020. Drought responses and their effects on radial stem growth of two co-occurring conifer species in the Mediterranean mountain range. *Ann. For. Sci.* 77, 105. <https://doi.org/10.1007/s13595-020-01007-2>.
- Hartmann, H., 2015. Carbon starvation during drought-induced tree mortality – are we chasing a myth? *J. Plant Hydraul.* 2, e005. <https://doi.org/10.20870/jph.2015.e005>.
- Hartmann, M., Brunner, I., Hagedorn, F., Bardgett, R.D., Stierli, B., Herzog, C., Chen, X., Zingg, A., Graf-Pannatier, E., Rigling, A., Frey, B., 2017. A decade of irrigation transforms the soil microbiome of a semi-arid pine forest. *Mol. Ecol.* 26, 1190–1206. <https://doi.org/10.1111/mec.13995>.
- Hartmann, H., Moura, C.F., Anderegg, W.R.L., Ruehr, N.K., Salmon, Y., Allen, C.D., Arndt, S.K., Breshears, D.D., Davi, H., Galbraith, D., Ruthrof, K.X., Wunder, J., Adams, H.D., Bloemen, J., Cailleret, M., Cobb, R., Gessler, A., Grams, T.E.E., Jansen, S., Kautz, M., Lloret, F., O'Brien, M., 2018. Research frontiers for improving our understanding of drought-induced tree and forest mortality. *New Phytol.* 218, 15–28. <https://doi.org/10.1111/nph.15048>.
- Hartmann, H., Bastos, A., Das, A.J., Esquivel-Muelbert, A., Hammond, W.M., Martínez-Vilalta, J., McDowell, N.G., Powers, J.S., Pugh, T.A.M., Ruthrof, K.X., Allen, C.D., 2022. Climate change risks to global forest health: emergence of unexpected events of elevated tree mortality worldwide. *Annu. Rev. Plant Biol.* 73, 673–702. <https://doi.org/10.1146/annurev-arplant-102820-012804>.
- Hemkemeyer, M., Christensen, B.T., Tebbe, C.C., Hartmann, M., 2019. Taxon-specific fungal preference for distinct soil particle size fractions. *Eur. J. Soil Biol.* 94, 103103. <https://doi.org/10.1016/j.ejsobi.2019.103103>.
- Hervé, M., 2023. Package ‘RVAideMemoire’ testing and plotting procedures for biostatistics v0.9-81-2 (version 0.9-81-2). <https://cran.r-project.org/web/packages/RVAideMemoire/index.html>.
- Hicke, J.A., Allen, C.D., Desai, A.R., Dietze, M.C., Hall, R.J., Hogg, E.H.T., Kashian, D.M., Moore, D., Raffa, K.F., Sturrock, R.N., Vogelmann, J., 2012. Effects of biotic disturbances on forest carbon cycling in the United States and Canada. *Glob. Chang. Biol.* 18, 7–34. <https://doi.org/10.1111/j.1365-2486.2011.02543.x>.
- Hicks, L.C., Lajtha, K., Rousk, J., 2021. Nutrient limitation may induce microbial mining for resources from persistent soil organic matter. *Ecology* 102, 1–16. <https://doi.org/10.1002/ecy.3328>.
- Homyak, P.M., Sickman, J.O., Miller, A.E., Melack, J.M., Meixner, T., Schimel, J.P., 2014. Assessing nitrogen-saturation in a seasonally dry chaparral watershed: limitations of traditional indicators of N-saturation. *Ecosystems* 17, 1286–1305. <https://doi.org/10.1007/s10021-014-9792-2>.
- Homyak, P.M., Allison, S.D., Huxman, T.E., Goulden, M.L., Treseder, K.K., 2017. Effects of drought manipulation on soil nitrogen cycling: a meta-analysis. *J. Geophys. Res. Biogeosci.* 122, 3260–3272. <https://doi.org/10.1002/2017JG004146>.
- Hopkins, A.J.M., Ruthrof, K.X., Fontaine, J.B., Matusick, G., Dundas, S.J., Hardy, G.E., 2018. Forest die-off following global-change-type drought alters rhizosphere fungal communities. *Environ. Res. Lett.* 13. <https://doi.org/10.1088/1748-9326/aad19>.
- Hothorn, T., Bretz, F., Westfall, P., Heiberger, R.M., Schuetzenmeister, A., Scheibe, S., 2023. Package ‘multcomp’. Simultaneous inference in general parametric models v.1.4-20 (version 1.4-20). <https://cran.r-project.org/web/packages/multcomp/multcomp.pdf>.
- Hunziker, S., Begert, M., Scherrer, S.C., Rigling, A., Gessler, A., 2022. Below average midsummer to early autumn precipitation evolved into the main driver of sudden scots pine vitality decline in the Swiss Rhône Valley. *Front. For. Glob. Chang.* 5. <https://doi.org/10.3389/ffgc.2022.874100>.
- Ivanova, A.A., Kulichevskaya, I.S., Merkel, A.Y., Toshchakov, S.V., Dedysh, S.N., 2016. High diversity of planctomycetes in soils of two lichen-dominated sub-Arctic ecosystems of northwestern Siberia. *Front. Microbiol.* 7, 1–13. <https://doi.org/10.3389/fmicb.2016.02065>.

- Jaeger, A.C.H., Hartmann, M., Six, J., Solly, E.F., 2023a. Contrasting sensitivity of soil bacterial and fungal community composition to one year of water limitation in Scots pine mesocosms. *FEMS Microbiol. Ecol.* 99 <https://doi.org/10.1093/femsec/fiad051>.
- Jaeger, A.C.H., Hartmann, M., Conz, R.F., Six, J., Solly, E.F., 2023b. Prolonged water limitation shifts the soil microbiome from copiotrophic to oligotrophic lifestyles in Scots pine mesocosms. *Environ. Microbiol. Rep.* (in press).
- Jenkins, J.C., Aber, J.D., Canham, C.D., 1999. Hemlock woolly adelgid impacts on community structure and N cycling rates in eastern hemlock forests. *Can. J. For. Res.* 29, 630–645. <https://doi.org/10.1139/x99-034>.
- Joergensen, R.G., Wichern, F., 2008. Quantitative assessment of the fungal contribution to microbial tissue in soil. *Soil Biol. Biochem.* 40, 2977–2991. <https://doi.org/10.1016/j.soilbio.2008.08.017>.
- Kaboré, O.D., Godreuil, S., Drancourt, M., 2020. Planctomycetes as host-associated bacteria: a perspective that holds promise for their future isolations, by mimicking their native environmental niches in clinical microbiology laboratories. *Front. Cell. Infect. Microbiol.* 10, 1–19. <https://doi.org/10.3389/fcimb.2020.519301>.
- Kim, S., Ahn, J., Lee, T., Weon, H., Hong, S., Seok, S., Whang, K., Kwon, S., 2013. *Reyranelia soli* sp. nov., isolated from forest soil, and emended description of the genus *Reyranelia* Pagnier et al. 2011. *Int. J. Syst. Evol. Microbiol.* 63, 3164–3167. <https://doi.org/10.1099/ijs.0.045922-0>.
- Kindt, R., 2008. BiodiversityR: package for community ecology and suitability analysis v2.14-4 (version 2.14-4). <https://www.worldagroforestry.org/output/tree-diversity-analysis>.
- Klein, T., Hartmann, H., 2018. Climate change drives tree mortality. *Science* (80-) 362, 758. <https://doi.org/10.1126/science.aav6508>.
- Kulichevskaya, I.S., Belova, S.E., Kevbrin, V.V., Dedysh, S.N., Zavarzin, G.A., 2007. Analysis of the bacterial community developing in the course of Sphagnum moss decomposition. *Microbiology* 76, 621–629. <https://doi.org/10.1134/S0026261707050165>.
- Kurz, W.A., Dymond, C.C., Stinson, G., Rampley, G.J., Neilson, E.T., Carroll, A.L., Ebata, T., Safranyik, L., 2008. Mountain pine beetle and forest carbon feedback to climate change. *Nature* 452, 987–990. <https://doi.org/10.1038/nature06777>.
- Langmead, B., Salzberg, S.L., 2012. Fast gapped-read alignment with bowtie 2. *Nat. Methods* 9, 357–359. <https://doi.org/10.1038/nmeth.1923>.
- Lee, H., Kim, D., Lee, S., Park, S., Yoon, J., Seong, C.N., Ka, J., 2017. *Reyranelia terrae* sp. nov., isolated from an agricultural soil, and emended description of the genus *Reyranelia*. *Int. J. Syst. Evol. Microbiol.* 67, 2031–2035. <https://doi.org/10.1099/ijsem.0.001913>.
- Legendre, P., Anderson, M.J., 1999. Distance-based redundancy analysis: testing multispecies responses in multifactorial ecological experiments. *Ecol. Monogr.* 69, 1–24. [https://doi.org/10.1890/0012-9615\(1999\)069\[0001:DBRATM\]2.0.CO;2](https://doi.org/10.1890/0012-9615(1999)069[0001:DBRATM]2.0.CO;2).
- Lindahl, B.D., Tunlid, A., 2015. Ectomycorrhizal fungi - potential organic matter decomposers, yet not saprotrophs. *New Phytol.* 205, 1443–1447. <https://doi.org/10.1111/nph.13201>.
- Lindahl, B.D., Ihrmark, K., Boberg, J., Trumbore, S.E., Högberg, P., Stenlid, J., Finlay, R. D., 2007. Spatial separation of litter decomposition and mycorrhizal nitrogen uptake in a boreal forest. *New Phytol.* 173, 611–620. <https://doi.org/10.1111/j.1469-8137.2006.01936.x>.
- Lindahl, B.D., Kyaschenko, J., Varenius, K., Clemmensen, K.E., Dahlberg, A., Karlton, E., Stendahl, J., 2021. A group of ectomycorrhizal fungi restricts organic matter accumulation in boreal forest. *Ecol. Lett.* 24, 1341–1351. <https://doi.org/10.1111/ele.13746>.
- Liu, Q., Peng, C., Schneider, R., Cyr, D., McDowell, N.G., Kneeshaw, D., 2023. Drought-induced increase in tree mortality and corresponding decrease in the carbon sink capacity of Canada's boreal forests from 1970 to 2020. *Glob. Chang. Biol.* 29, 2274–2285. <https://doi.org/10.1111/gcb.16599>.
- Lladó, S., López-Mondéjar, R., Baldrian, P., 2017. Forest soil bacteria: diversity, involvement in ecosystem processes, and response to global change. *Microbiol. Mol. Biol. Rev.* 81, 1–27. <https://doi.org/10.1128/mmb.0063-16>.
- Lloret, F., Mattana, S., Curiel Yuste, J., 2015. Climate-induced die-off affects plant-soil-microbe ecological relationship and functioning. *FEMS Microbiol. Ecol.* 91, 1–12. <https://doi.org/10.1093/femsec/fiu014>.
- MacAllister, S., Mencuccini, M., Sommer, U., Engel, J., Hudson, A., Salmon, Y., Dexter, K. G., 2019. Drought-induced mortality in Scots pine: opening the metabolic black box. *Tree Physiol.* 39, 1358–1370. <https://doi.org/10.1093/treephys/tpz049>.
- Martens-Habbena, W., Berube, P.M., Urakawa, H., De La Torre, J.R., Stahl, D.A., 2009. Ammonia oxidation kinetics determine niche separation of nitrifying Archaea and Bacteria. *Nature* 461, 976–979. <https://doi.org/10.1038/nature08465>.
- Martin, M., 2011. Cutadapt removes adapter sequences from high-throughput sequencing reads. *EMBnet journal* 17, 10. <https://doi.org/10.14806/ej.17.1.200>.
- Martínez-Vilalta, J., Mencuccini, M., Vayreda, J., Retana, J., 2010. Interspecific variation in functional traits, not climatic differences among species ranges, determines demographic rates across 44 temperate and Mediterranean tree species. *J. Ecol.* 98, 1462–1475. <https://doi.org/10.1111/j.1365-2745.2010.01718.x>.
- Martiny, J.B.H., Martiny, A.C., Weihe, C., Lu, Y., Berlemont, R., Brodie, E.L., Goulden, M. L., Treseder, K.K., Allison, S.D., 2017. Microbial legacies alter decomposition in response to simulated global change. *ISME J.* 11, 490–499. <https://doi.org/10.1038/ismej.2016.122>.
- Mayer, M., Matthews, B., Sandén, H., Katzensteiner, K., Hagedorn, F., Gorfer, M., Berger, H., Berger, T.W., Godbold, D.L., Rewald, B., 2023. Soil fertility determines whether ectomycorrhizal fungi accelerate or decelerate decomposition in a temperate forest. *New Phytol.* 325–339. <https://doi.org/10.1111/nph.18930>.
- McDowell, N.G., 2011. Mechanisms linking drought, hydraulics, carbon metabolism, and vegetation mortality. *Plant Physiol.* 155, 1051–1059. <https://doi.org/10.1104/pp.110.170704>.
- McDowell, N.G., Pockman, W.T., Allen, C.D., Breshears, D.D., Cobb, N., Kolb, T., Plaut, J., Sperry, J., West, A., Williams, D.G., Yepez, E.A., 2008. Mechanisms of plant survival and mortality during drought: why do some plants survive while others succumb to drought? *New Phytol.* 178, 719–739. <https://doi.org/10.1111/j.1469-8137.2008.02436.x>.
- McDowell, N.G., Fisher, R.A., Xu, C., Domec, J.C., Hölttä, T., Mackay, D.S., Sperry, J.S., Boutz, A., Dickman, L., Gehres, N., Limousin, J.M., Macalady, A., Martínez-Vilalta, J., Mencuccini, M., Plaut, J.A., Ogée, J., Pangle, R.E., Rasse, D.P., Ryan, M. G., Sevanto, S., Waring, R.H., Williams, A.P., Yepez, E.A., Pockman, W.T., 2013. Evaluating theories of drought-induced vegetation mortality using a multimodel-experiment framework. *New Phytol.* 200, 304–321. <https://doi.org/10.1111/nph.12465>.
- McDowell, N.G., Sapes, G., Pivovarov, A., Adams, H.D., Allen, C.D., Anderegg, W.R.L., Arend, M., Breshears, D.D., Brodrick, T., Choat, B., Cochard, H., De Cáceres, M., De Kauwe, M.G., Grossiord, C., Hammond, W.M., Hartmann, H., Hoch, G., Kahmen, A., Klein, T., Mackay, D.S., Mantova, M., Martínez-Vilalta, J., Medlyn, B.E., Mencuccini, M., Nardini, A., Oliveira, R.S., Sala, A., Tissue, D.T., Torres-Ruiz, J.M., Trowbridge, A.M., Trugman, A.T., Wiley, E., Xu, C., 2022. Mechanisms of woody-plant mortality under rising drought, CO<sub>2</sub> and vapour pressure deficit. *Nat. Rev. Earth Environ.* 3, 294–308. <https://doi.org/10.1038/s43017-022-00272-1>.
- Meisner, A., Jacquiod, S., Snoek, B.L., Ten Hooven, F.C., van der Putten, W.H., 2018. Drought legacy effects on the composition of soil fungal and prokaryote communities. *Front. Microbiol.* 9, 1–12. <https://doi.org/10.1111/nph.12857>.
- Meyer, K., 1989. Restricted maximum likelihood to estimate variance components for animal models with several random effects using a derivative-free algorithm. *Genet. Sel. Evol.* 21, 317. <https://doi.org/10.1186/1297-9686-21-3-317>.
- Michas, A., Pastore, G., Chiba, A., Grafe, M., Clausen, S., Polle, A., Schloter, M., Spohn, M., Schulz, S., 2021. Phosphorus availability alters the effect of tree girdling on the diversity of phosphorus solubilizing soil bacterial communities in temperate beech forests. *Front. For. Glob. Chang.* 4, 1–9. <https://doi.org/10.3389/ffgc.2021.696983>.
- Modi, D., Simard, S., Bérubé, J., Lavkulich, L., Hamelin, R., Grayston, S.J., 2021. Long-term effects of stump removal and tree species composition on the diversity and structure of soil fungal communities. *FEMS Microbiol. Ecol.* 96, 1–12. <https://doi.org/10.1093/FEMSEC/FIAA061>.
- Mueller, R.C., Scudder, C.M., Porter, M.E., Talbot Trotter, R., Gehring, C.A., Whitham, T. G., 2005. Differential tree mortality in response to severe drought: evidence for long-term vegetation shifts. *J. Ecol.* 93, 1085–1093. <https://doi.org/10.1111/j.1365-2745.2005.01042.x>.
- Nara, K., 2009. Spores of ectomycorrhizal fungi: ecological strategies for germination and dormancy. *New Phytol.* 181, 245–248. <https://doi.org/10.1111/j.1469-8137.2008.02691.x>.
- Nave, L.E., Gough, C.M., Maurer, K.D., Bohrer, G., Hardiman, B.S., Le Moine, J., Munoz, A.B., Nadelhoffer, K.J., Sparks, J.P., Strahm, B.D., Vogel, C.S., Curtis, P.S., 2011. Disturbance and the resilience of coupled carbon and nitrogen cycling in a north temperate forest. *J. Geophys. Res.* 116, G04016 <https://doi.org/10.1029/2011JG001758>.
- Nguyen, N.H., Song, Z., Bates, S.T., Branco, S., Tedersoo, L., Menke, J., Schilling, J.S., Kennedy, P.G., 2016. FUNGuild: an open annotation tool for parsing fungal community datasets by ecological guild. *Fungal Ecol.* 20, 241–248. <https://doi.org/10.1016/j.funeco.2015.06.006>.
- Nilsson, R.H., Anslan, S., Bahram, M., Wurzbacher, C., Baldrian, P., Tedersoo, L., 2019a. Mycobiome diversity: high-throughput sequencing and identification of fungi. *Nat. Rev. Microbiol.* 17, 95–109. <https://doi.org/10.1038/s41579-018-0116-y>.
- Nilsson, R.H., Larsson, K.H., Taylor, A.F.S., Bengtsson-Palme, J., Jeppesen, T.S., Schigel, D., Kennedy, P., Picard, K., Glöckner, F.O., Tedersoo, L., Saar, I., Kõljalg, U., Abarenkov, K., 2019b. The UNITE database for molecular identification of fungi: handling dark taxa and parallel taxonomic classifications. *Nucleic Acids Res.* 47, D259–D264. <https://doi.org/10.1093/nar/gky1022>.
- Oksanen, J., Simpson, G.L., Blanchet, F.G., Solyomos, P., Stevens, M.H.H., Szoecs, E., Wagner, H., Barbour, M., Bedward, M., Bolker, B., Borcard, D., Carvalho, G., Chirico, M., Durand, S., Beatriz, H., Evangelista, A., Friendly, M., Hannigan, G., Hill, M.O., Lahti, L., Mcglinn, D., Ribeiro, E., Smith, T., Stier, A., Ter, C.J.F., 2022. Package 'vegan'. Community ecology package v2.6-4 (version 2.6-4). <https://github.com/vegandevs/vegan>.
- Oliva, J., Stenlid, J., Martínez-Vilalta, J., 2014. The effect of fungal pathogens on the water and carbon economy of trees: implications for drought-induced mortality. *New Phytol.* 203, 1028–1035. <https://doi.org/10.1111/nph.12857>.
- Oren, A., Xu, X.-W., 2014. The family hyphomicrobiaceae. In: *The Prokaryotes*. Springer Berlin Heidelberg, Berlin, Heidelberg, pp. 247–281. [https://doi.org/10.1007/978-3-642-30197-1\\_257](https://doi.org/10.1007/978-3-642-30197-1_257).
- Parada, A.E., Needham, D.M., Fuhrman, J.A., 2016. Every base matters: assessing small subunit rRNA primers for marine microbiomes with mock communities, time series and global field samples. *Environ. Microbiol.* 18, 1403–1414. <https://doi.org/10.1111/1462-2920.13023>.
- Parker, S.S., Schimel, J.P., 2011. Soil nitrogen availability and transformations differ between the summer and the growing season in a California grassland. *Appl. Soil Ecol.* 48, 185–192. <https://doi.org/10.1016/j.apsoil.2011.03.007>.
- Pinheiro, J., Bates, D., DebRoy, S., Sarkar, D., 2022. Package 'nlme'. Linear and nonlinear mixed effects models v3.1-160 (version 3.1-160). <https://svn.r-project.org/R/packages/trunk/nlme/>.
- Prescott, C.E., 2010. Litter decomposition: what controls it and how can we alter it to sequester more carbon in forest soils? *Biogeochemistry* 101, 133–149. <https://doi.org/10.1007/s10533-010-9439-0>.
- Pretzsch, H., Rüdiger, R., Hans, G., Klemmt, J., Ordóñez, C., 2022. Tracing drought effects from the tree to the stand growth in temperate and Mediterranean forests:

- insights and consequences for forest ecology and management. *Eur. J. For. Res.* 141, 727–751. <https://doi.org/10.1007/s10342-022-01451-x>.
- Quast, C., Pruesse, E., Yilmaz, P., Gerken, J., Schweer, T., Yarza, P., Peplies, J., Glöckner, F.O., 2013. The SILVA ribosomal RNA gene database project: improved data processing and web-based tools. *Nucleic Acids Res.* 41, 590–596. <https://doi.org/10.1093/nar/gks1219>.
- R Core Team, 2023. R: A Language and Environment for Statistical Computing. R Foundation for Statistical Computing, Vienna, Austria. <https://www.R-project.org/>.
- Rajala, T., Peltoniemi, M., Hantula, J., Mäkipää, R., Pennanen, T., 2011. RNA reveals a succession of active fungi during the decay of Norway spruce logs. *Fungal Ecol.* 4, 437–448. <https://doi.org/10.1016/j.funeco.2011.05.005>.
- Rasheed, M.U., Kivimäenpää, M., Kasurinen, A., 2021. Emissions of biogenic volatile organic compounds (BVOCs) from the rhizosphere of Scots pine (*Pinus sylvestris*) seedlings exposed to warming, moderate N addition and bark herbivory by large pine weevil (*Hyllobius abietis*). *Plant and Soil* 463, 379–394. <https://doi.org/10.1007/s11104-021-04888-y>.
- Rigling, A., Bigler, C., Eilmann, B., Feldmeyer-Christe, E., Gimmi, U., Ginzler, C., Graf, U., Mayer, P., Vacchiano, G., Weber, P., Wohlgemuth, T., Zweifel, R., Dobbertin, M., 2013. Driving factors of a vegetation shift from Scots pine to pubescent oak in dry Alpine forests. *Glob. Chang. Biol.* 19, 229–240. <https://doi.org/10.1111/gcb.12038>.
- Rodríguez, A., Curiel Yuste, J., Rey, A., Durán, J., García-Camacho, R., Gallardo, A., Valladares, F., 2017. Holm oak decline triggers changes in plant succession and microbial communities, with implications for ecosystem C and N cycling. *Plant and Soil* 414, 247–263. <https://doi.org/10.1007/s11104-016-3118-4>.
- Rodríguez-Ramos, J.C., Cale, J.A., Cahill, J.F., Simard, S.W., Karst, J., Erbilgin, N., 2021. Changes in soil fungal community composition depend on functional group and forest disturbance type. *New Phytol.* 229, 1105–1117. <https://doi.org/10.1111/nph.16749>.
- Rognes, T., Flouri, T., Nichols, B., Quince, C., Mahé, F., 2016. VSEARCH: a versatile open source tool for metagenomics. *PeerJ* 2016, 1–22. <https://doi.org/10.7717/peerj.2584>.
- Rosenberg, E., De Long, E.F., Lory, S., Stackebrandt, E., Thompson, F., 2014. The Prokaryotes: Other Major Lineages of Bacteria and the Archaea, fourth ed. Springer, Berlin, Heidelberg. <https://doi.org/10.1007/978-3-642-38954-2>.
- RStudio Team, 2023. RStudio: Integrated Development Environment for R. RStudio, PBC, Boston, MA (URL). <http://www.rstudio.com/>.
- Sánchez-Salguero, R., Navarro-Cerrillo, R.M., Camarero, J.J., Fernández-Cancio, Á., 2012. Selective drought-induced decline of pine species in southeastern Spain. *Clim. Chang.* 113, 767–785. <https://doi.org/10.1007/s10584-011-0372-6>.
- Schimel, J., Balsler, T.C., Wallenstein, M., 2007. Microbial stress-response physiology and its implications for ecosystem function. *Ecology* 88, 1386–1394. <https://doi.org/10.1890/06-0219>.
- Sevanto, S., McDowell, N.G., Dickman, L.T., Pangle, R., Pockman, W.T., 2014. How do trees die? A test of the hydraulic failure and carbon starvation hypotheses. *Plant Cell Environ.* 37, 153–161. <https://doi.org/10.1111/pce.12141>.
- Shao, S., Wurzbarger, N., Sulman, B., Hicks Pries, C., 2023. Ectomycorrhizal effects on decomposition are highly dependent on fungal traits, climate, and litter properties: a model-based assessment. *Soil Biol. Biochem.* 184, 109073 <https://doi.org/10.1016/j.soilbio.2023.109073>.
- Sherrod, L.A., Dunn, G., Peterson, G.A., Kolberg, R.L., 2002. Inorganic carbon analysis by modified pressure-calimeter method. *Soil Sci. Soc. Am. J.* 66, 299–305. <https://doi.org/10.2136/sssaj2002.2990>.
- Six, J., Frey, S.D., Thiet, R.K., Batten, K.M., 2006. Bacterial and fungal contributions to carbon sequestration in agroecosystems. *Soil Sci. Soc. Am. J.* 70, 555–569. <https://doi.org/10.2136/sssaj2004.0347>.
- Solly, E.F., Schöning, I., Herold, N., Trumbore, S.E., Schrupf, M., 2015. No depth-dependence of fine root litter decomposition in temperate beech forest soils. *Plant and Soil* 393, 273–282. <https://doi.org/10.1007/s11104-015-2492-7>.
- Solly, E.F., Jaeger, A.C.H., Barthel, M., Werner, R.A., Zürcher, A., Hagedorn, F., Six, J., Hartmann, M., 2023. Water limitation intensity shifts carbon allocation dynamics in Scots pine mesocosms. *Plant and Soil*. <https://doi.org/10.1007/s11104-023-06093-5>.
- Soong, J.L., Fuchslueger, L., Marañón-Jimenez, S., Torn, M.S., Janssens, I.A., Penuelas, J., Richter, A., 2020. Microbial carbon limitation: the need for integrating microorganisms into our understanding of ecosystem carbon cycling. *Glob. Chang. Biol.* 26, 1953–1961. <https://doi.org/10.1111/gcb.14962>.
- Storey, J.D., Tibshirani, R., 2003. Statistical significance for genomewide studies. *Proc. Natl. Acad. Sci. U. S. A.* 100, 9440–9445. <https://doi.org/10.1073/pnas.1530509100>.
- Storey, J.D., Bass, A.J., Dabney, A., Robinson, D., Warnes, G., 2023. Package ‘qvalue’ Q-value estimation for false discovery rate control v2.27.0 (Version 2.27.0). <https://github.com/StoreyLab/qvalue>.
- Štursová, M., Zifčáková, L., Leigh, M.B., Burgess, R., Baldrian, P., 2012. Cellulose utilization in forest litter and soil: identification of bacterial and fungal decomposers. *FEMS Microbiol. Ecol.* 80, 735–746. <https://doi.org/10.1111/j.1574-6941.2012.01343.x>.
- Štursová, M., Šnajdr, J., Cajthaml, T., Bárta, J., Santrůčková, H., Baldrian, P., 2014. When the forest dies: the response of forest soil fungi to a bark beetle-induced tree dieback. *ISME J.* 8, 1920–1931. <https://doi.org/10.1038/ismej.2014.37>.
- Tecon, R., Or, D., 2017. Biophysical processes supporting the diversity of microbial life in soil. *FEMS Microbiol. Rev.* 41, 599–623. <https://doi.org/10.1093/femsre/fux039>.
- Tedersoo, L., Lindahl, B., 2016. Fungal identification biases in microbiome projects. *Environ. Microbiol. Rep.* 8, 774–779. <https://doi.org/10.1111/1758-2229.12438>.
- Tedersoo, L., May, T.W., Smith, M.E., 2010. Ectomycorrhizal lifestyle in fungi: global diversity, distribution, and evolution of phylogenetic lineages. *Mycorrhiza* 20, 217–263. <https://doi.org/10.1007/s00572-009-0274-x>.
- Tedersoo, L., Bahram, M., Pöhlme, S., Kõljalg, U., Yorou, N.S., Wijesundera, R., Ruiz, L.V., Vasco-Palacios, A.M., Thu, P.Q., Suijja, A., Smith, M.E., Sharp, C., Saluveer, E., Saitta, A., Rosas, M., Riit, T., Ratkowsky, D., Pritsch, K., Pöhlmaa, K., Piepenbring, M., Phosri, C., Peterson, M., Parts, K., Pärtel, K., Otsing, E., Nohra, E., Njounkou, A.L., Nilsson, R.H., Morgado, L.N., Mayor, J., May, T.W., Majuakim, L., Lodge, D.J., Lee, S.S., Larsson, K.-H., Kohout, P., Hosaka, K., Hiiesalu, I., Henkel, T. W., Harend, H., Guo, L., Greslebin, A., Grelet, G., Geml, J., Gates, G., Dunstan, W., Dunk, C., Drenkhan, R., Dearnaley, J., De Kesel, A., Dang, T., Chen, X., Buegger, F., Brearley, F.Q., Bonito, G., Anslan, S., Abell, S., Abarenkov, K., 2014. Global diversity and geography of soil fungi. *Science* (80-) 346. <https://doi.org/10.1126/science.1256688>.
- Tóth, Z., Táncsics, A., Kriszt, B., Kröel-Dulay, G., Ónodi, G., Hornung, E., 2017. Extreme effects of drought on composition of the soil bacterial community and decomposition of plant tissue. *Eur. J. Soil Sci.* 68, 504–513. <https://doi.org/10.1111/ejss.12429>.
- Trivedi, P., Singh, B.P., Singh, B.K., 2018. 2018. Chapter 1 - soil carbon: introduction, importance, status, threat, and mitigation. In: Singh, Brajesh K. (Ed.), *Soil Carbon Storage: Modulators, Mechanisms and Modeling*. Academic Press, Elsevier Inc., pp. 1–28. <https://doi.org/10.1016/B978-0-12-812766-7.00001-9>.
- Tunlid, A., Floudas, D., Op De Beeck, M., Wang, T., Persson, P., 2022. Decomposition of soil organic matter by ectomycorrhizal fungi: mechanisms and consequences for organic nitrogen uptake and soil carbon stabilization. *Front. For. Glob. Chang.* 5, 1–9. <https://doi.org/10.3389/ffgc.2022.934409>.
- Usman, M., Ho-Plágaro, T., Frank, H.E.R., Calvo-Polanco, M., Gaillard, I., Garcia, K., Zimmermann, S.D., 2021. Mycorrhizal symbiosis for better adaptation of trees to abiotic stress caused by climate change in temperate and boreal forests. *Front. For. Glob. Chang.* 4 <https://doi.org/10.3389/ffgc.2021.742392>.
- Vainio, E.J., Hantula, J., 2000. Direct analysis of wood-inhabiting fungi using denaturing gradient gel electrophoresis of amplified ribosomal DNA. *Mycol. Res.* 104, 927–936. <https://doi.org/10.1017/S0953756200002471>.
- van Niftrik, L., Jetten, M.S.M., 2012. Anaerobic ammonium-oxidizing bacteria: unique microorganisms with exceptional properties. *Microbiol. Mol. Biol. Rev.* 76, 585–596. <https://doi.org/10.1128/MMBR.05025-11>.
- Veselá, P., Vasutová, M., Edwards-Jonášová, M., Cudlín, P., 2019. Soil fungal community in Norway spruce forests under bark beetle attack. *Forests* 10, 1–14. <https://doi.org/10.3390/f10020109>.
- Voriskova, J., Baldrian, P., 2013. Fungal community on decomposing leaf litter undergoes rapid successional changes. *ISME J.* 7, 477–486. <https://doi.org/10.1038/ismej.2012.116>.
- Vos, M., Wolf, A.B., Jennings, S.J., Kowalchuk, G.A., 2013. Micro-scale determinants of bacterial diversity in soil. *FEMS Microbiol. Rev.* 37, 936–954. <https://doi.org/10.1111/1574-6976.12023>.
- Ward, J.H., 1963. Hierarchical grouping to optimize an objective function. *J. Am. Stat. Assoc.* 58, 236. <https://doi.org/10.2307/2282967>.
- Warnes, G., Bolker, B., Huber, W., Lumley, T., Maechler, M., Magnusson, A., Moeller, S., 2022. Package ‘gplots’. Various R programming tools for plotting data v3.0.1.2 (Version 3.1.0.2). <https://github.com/taigalili/gplots>.
- Weemstra, M., Mommer, L., Visser, E.J.W., van Ruijven, J., Kuyper, T.W., Mohren, G.M. J., Sterck, F.J., 2016. Towards a multidimensional root trait framework: a tree root review. *New Phytol.* 211, 1159–1169. <https://doi.org/10.1111/nph.14003>.
- Wickham, H., Chang, W., Henry, L., Pedersen, T.L., Takahashi, K., Wilke, C., Woo, K., Yutani, H., Dunnington, D., 2023. R package ‘ggplot2’ v3.4.4. Elegant graphics for data analysis. <https://ggplot2.tidyverse.org/>.
- Xia, M., Guo, D., Pregitzer, K.S., 2010. Ephemeral root modules in fraxinus mandshurica. *New Phytol.* 188, 1065–1074. <https://doi.org/10.1111/j.1469-8137.2010.03423.x>.
- Xiong, Y., D’Atri, J.J., Fu, S., Xia, H., Seastedt, T.R., 2011. Rapid soil organic matter loss from forest dieback in a subalpine coniferous ecosystem. *Soil Biol. Biochem.* 43, 2450–2456. <https://doi.org/10.1016/j.soilbio.2011.08.013>.
- Yuste, J.C., Penuelas, J., Estiarte, M., Garcia-Mas, J., Mattana, S., Ogaya, R., Pujol, M., Sardans, J., 2011. Drought-resistant fungi control soil organic matter decomposition and its response to temperature. *Glob. Chang. Biol.* 17, 1475–1486. <https://doi.org/10.1111/j.1365-2486.2010.02300.x>.
- Yuste, J.C., Barba, J., Fernandez-Gonzalez, A.J., Fernandez-Lopez, M., Mattana, S., Martinez-Vilalta, J., Nolis, P., Lloret, F., 2012. Changes in soil bacterial community triggered by drought-induced gap succession preceded changes in soil C stocks and quality. *Ecol. Evol.* 2, 3016–3031. <https://doi.org/10.1002/ece3.409>.
- Zak, D.R., Pellitier, P.T., Argiroff, W.A., Castillo, B., James, T.Y., Nave, L.E., Averill, C., Beidler, K.V., Bhatnagar, J., Blesh, J., Classen, A.T., Craig, M., Fernandez, C.W., Gundersen, P., Johansen, R., Koide, R.T., Lilleskov, E.A., Lindahl, B.D., Nadelhoffer, K.J., Phillips, R.P., Tunlid, A., 2019. Exploring the role of ectomycorrhizal fungi in soil carbon dynamics. *New Phytol.* 223, 33–39. <https://doi.org/10.1111/nph.15679>.
- Zeller, B., Liu, J., Buchmann, N., Richter, A., 2008. Tree girdling increases soil N mineralisation in two spruce stands. *Soil Biol. Biochem.* 40, 1155–1166. <https://doi.org/10.1016/j.soilbio.2007.12.009>.
- Zhao, M., Running, S.W., 2010. Drought-induced reduction in global terrestrial net primary production from 2000 through 2009. *Science* (80-) 329, 940–943. <https://doi.org/10.1126/science.1192666>.